Recent advances on $Mg_2Si_{1-x}Sn_x$ materials for thermoelectric generation

Mohamed Bashir Ali Bashir [a], Suhana Mohd Said [b,*], Mohd Faizul Mohd Sabri [a], Dhafer Abdulameer Shnawah [a], Mohamed Hamid Elsheikh [a,c]

[a] Department of Mechanical Engineering, University of Malaya, 50603 Kuala Lumpur, Malaysia
[b] Department of Electrical Engineering, University of Malaya, 50603 Kuala Lumpur, Malaysia
[c] Department of Mechanical Engineering, University of Bahri, 13104 Khartoum, Sudan

A B S T R A C T

Thermoelectric generators (TEGs) have been identified as a viable technology for waste energy harvesting, from heat into electricity. Key to successful realization of this technology on a commercial scale lies largely with the thermoelectric material which drives this technology. While bismuth telluride based TEGs dominate the current market, liabilities such as toxicity, depletion of raw resources and high production costs have triggered the search for alternative thermoelectric materials. One of the contenders as thermoelectric materials in the mid-temperature range is the family of Mg–Mn silicides, given the advantages of abundance of raw resources, relatively high thermoelectric performance, lowered production costs, and environmental compatibility. In this paper, the thermoelectric performance of this class of materials is first reviewed through the key thermoelectric parameters: thermal and electrical conductivity, Seebeck coefficient and power factor. The development fabrication processes for this class of materials, using nanostructuring and element doping strategies, are then elaborated. Finally, comments on the thermoelectric applications and device efficiency are made within the context of this material.

© 2014 Elsevier Ltd. All rights reserved.

Contents

* Corresponding author. Tel.: +60 379675399; Fax: +60 379675317.
E-mail address: smsaid@um.edu.my (S. Mohd Said).

1. Introduction

Global energy consumption has increased exponentially in the last century, with the majority of the energy being supplied by fossil fuels [1–5] such as petroleum, natural gas, and coal [6,7]. The burning of fossil fuels and consequent emission of greenhouse gases have an adverse impact on the environment, in terms of global warming, climate change and pollution [8–13]. In heat engines, only approximately 30–40% of the fossil fuels burnt are utilized as useful energy, while the rest is wasted heat in the form of exhaust gases and friction [14]. The International Energy Agency indicated that the electricity and heat production sectors produce about 32% of the global greenhouse gas emissions, which is equivalent to 49.5 gigatonnes of carbon dioxide in 2010. In the automobile sector, Alam and Ramakrishna reported that 191 million vehicles in US have dissipated about 66% of energy as wasted heat, which amount to a total of approximately 36 TWh/year of emissions to the environment [15].

Thermoelectric generators (TEGs) are considered as a leading technology for waste heat harvesting. The introduction of TEGs is intended to mitigate the effect of fuel consumption, and consequently reduce CO_2 emissions. TEGs have a potential of reducing 40 million tons of CO_2 emissions per year, based on a TEG efficiency of 20% [16]. Collectively, TEGs are thought to be applicable in harvesting waste heat from the industrial, transportation and domestic sectors [17–19]. Thermoelectric is an energy conversion technology which allows solid state conversion of thermal energy directly into electrical energy and vice versa. TEG modules are scalable and thus applicable in systems from the miniature miliwatt level (body heat and portable electronics devices) to large-scale megawatt applications such as in the steelworks and cement industries [20–22]. There is currently a concerted effort to reduce energy consumption and environmental emissions through TEG technology.

Recognizing the potential of TEGs as an energy harvesting technology, nations and industrial sectors have recognized the value of TEG technology as a large-scale programme. Its extensive implementation is crucial for energy planning and policies, in terms of cost savings, resource optimization, and environmental protection on a national and global scale [23–27]. For example, the Japanese government has embarked on a 30-year thermoelectric roadmap (2010–2040). This roadmap starts from the synthesis of nanostructured thermoelectric materials to eventual implementation of TEGs in smart grid cogeneration systems, and large-scale centralized TEG systems, as shown in Fig. 1 [28]. On a similar scale, Germany is targeting an era of renewable energies by 2050. A key component of this programme is the driving of thermoelectric

technologies through a "nanothermoelectrics" research programme (2011–2014) [29]. In industry, the BMW group has embarked on a 20-year thermoelectric roadmap as shown in Fig. 2 which is expected to result in approximately 10% improvement in vehicle fuel economy through thermoelectric waste heat recovery [30]. Similarly, the US Department of Energy has initiated a "FreedomCar" programme for trucks and vehicles which utilize the TEGs to waste heat from automobile engines, with the aim of improving fuel economy by 10% [31].

The key to achieving highly efficient TEGs are through the development of highly efficient thermoelectric materials. However, other criteria such as cost, ease of fabrication, availability of raw resources, toxicity and environmental impact and end of life processing also play an important role in the selection of thermoelectric material for TEGs [32,33]. Currently, the high cost of the materials ($7–$42 per Watt) and the relatively low efficiency of about (6–8%) of the thermoelectric generators limit the development of TEG applications on a large scale [34,35]. However, TEGs do have the advantages of having no moving parts, are silent and reliable with a long lifetime (typically more than 100,000 h), and in most cases, environmentally compatible. Furthermore, they are compact and scalable, and thus suited to a wide range of applications.

Thermoelectric material performance is defined by their dimensionless figure of merit, ZT, as shown in Eq. (1), and where a high ZT would result from maximizing the Seebeck coefficient S and electrical conductivity σ, and minimizing the thermal conductivity K [36]:

$$ZT = S^2 T\sigma/K \tag{1}$$

Existing TEG systems rely on materials generally with a ZT of 1.3–1.5 in the medium and wide temperature range applications, but true commercial viability can only be achieved for $ZT > 4$ [37]. Novel classes of materials have been developed in thermoelectric such as skutterudites, clathrates, chalcogenides, and silicides. For example, in the family of silicides, magnesium silicide thermoelectric materials offer a relatively high figure of merit of approximately 1.3 and lower cost thermoelectric materials.

Currently, in commercial applications, the leading materials used in TEGs are bismuth telluride and members of the skutterudite family [38,39]. However, silicides such as magnesium silicide are gaining interest as favorable candidates for thermoelectric materials, given their advantages of relatively high figure of merit, high carrier mobility, lower cost, ecological friendliness, mechanical strength, chemical strength and abundance of raw materials. Generally, for magnesium silicide, the ZT is comparable to bismuth telluride, in the range of 1.0–1.3 [40,41], but has the advantage of lowered cost ($Mg_2Si_{0.6}Sn_{0.4}$ 4.04 $/kg) compared with conventional bismuth telluride ($Bi_{0.52}Sb_{1.48}Te_3$ 125 $/kg) [42]. Furthermore, Sano et al. [43], in their technical report, suggested that the
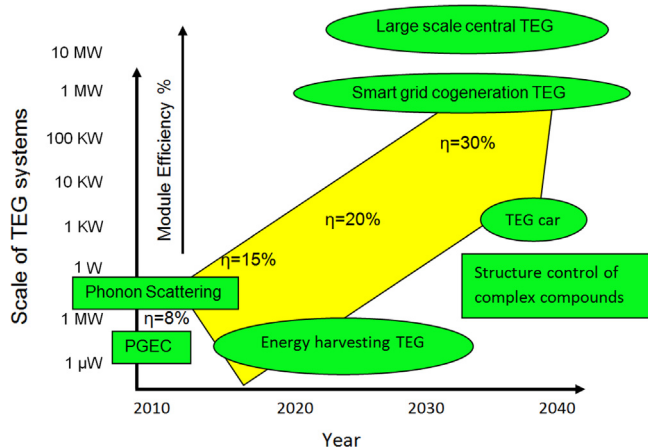

Fig. 1. The TEG systems applications development roadmap [28].
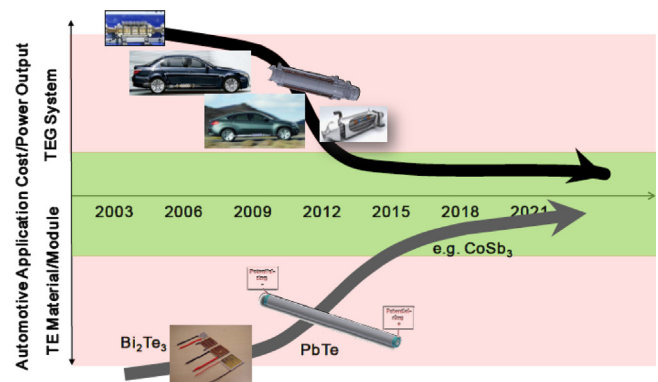

Fig. 2. Thermoelectric generators roadmap of the BMW group [30].

selling prices of bismuth telluride thermoelectric modules range from $7 to $42 per Watt, while Mg_2Sn has almost the same performance but costs less than a quarter of the price [44].

The figure of merit may also be evaluated through another material parameter, A' (where $A' \alpha ZT$) which can be described by the following equation [45]:

$$A' \approx (T/300)(m^*/m)^{\wedge 2/3}(\mu/K_L) \tag{2}$$

where $m*$ is the carrier effective mass, μ is the mobility in cm^2 V/s, and K_L is the lattice thermal conductivity in mW/cm K. High carrier mobility will contribute directly to electrical conductivity. Mg_2Si has been shown to possess a significantly high carrier mobility at room temperature, i.e. 406 cm^2/V s for n-type and 56 cm^2/V s for p-type [46], compared to $Ag_xSb_{2-x}Te_{3-x}$ which is in the range of 14–144 cm^2/V s [47], Zn_3P_2 (177 cm^2/V s), and $MnSi_{1.73}$ which is about 130–200 cm^2/V s [20]. Furthermore, Mg_2X (X=Si, Sn, Ge) compounds have a larger value of material factor A' (3.7–14) compared to other conventional thermoelectric silicide materials such as silicon germanium SiGe (1.2–2.6), manganese silicide 1.4 and iron silicide β-$FeSi_2$ (0.05–0.8) [45,48,49]. These factors mentioned above have indicated that the Mg_2 (Si, Sn, Ge) group is a viable candidate for commercial thermoelectric materials, particularly in the medium temperature range 500–900 K.

This paper discusses the environmental compatibility of thermoelectric materials Mg_2(Si–Sn) as energy conversion materials. Moreover, the thermoelectric potential of these materials will be discussed in the context of the governing parameters: thermal conductivity, electrical conductivity, Seebeck coefficient and power factor. Subsequently, strategies to improve the thermoelectric performance of these materials through nanostructuring and doping will be elaborated. To conclude the review, discussion on the potential applications and device efficiency as thermoelectric waste heat harvesters will be provided.

2. Thermoelectric properties

2.1. Thermal conductivity

The thermal conductivity K is related to the transfer of heat through materials, either by the charge carrier (electrons or holes), lattice waves (phonons), electromagnetic waves, spin waves, or other excitations. Normally, the total thermal conductivity K can be written by the Fourier Law, 1822 [50]:

$$q = -K \cdot (dT/dx) \tag{3}$$

where q is the heat current density flowing through the material, dT/dx is the temperature gradient in the material, and the negative sign indicates that the heat flows from the hot to the cold end. A reduction of thermal conductivity K is desirable to increase ZT and may be achieved by phonon scattering. Phonons are an important source of scattering in heat transfer, and its scattering in solid solutions is defined by the local changes in density associated with the different atoms [51]. Thermal conductivity through a crystalline lattice may be described in terms of its lattice vibration and electron contributions, as follows [52]:

$$K = K_L + K_e \tag{4}$$

where K_L and K_e are the lattice vibration and electron thermal conductivities, respectively. The lattice thermal conductivity component can be described by following equation [53]:

$$K_{Lattice} = 1/3 (C_v V_s \lambda_{ph}) \tag{5}$$

where C_v is the heat capacity (specific heat of the lattice), V_s is the sound velocity, and λ_{ph} is the phonon mean free path (mfp). In metals, electron carriers are mainly responsible for heat transfer, carry the majority of the heat, while in insulators lattice waves dominate the heat transfer mechanism, and in materials heat conduction is attributed to both electron carriers and lattice waves [54].

Materials with very low thermal conductivities are required to improve the performance of thermoelectric material. In thermoelectric materials, there are several ways to reduce K without affecting S and σ of materials, such as the use semiconductors of high atomic weight [55]; the use of complex structures with heavy atomic weight to enhance the phonon scattering, reduce the frequency of vibration, and formation of a polycrystalline nanostructure. Low thermal conductivity materials which have complex structures such as skutterudites, clathrates, half-Heusler alloys, chalcogenides and novel oxides are the focus for high efficiency thermoelectric materials [56]. For example, skutterudites, as shown in Fig. 3, can be filled with heavy atoms acting as "rattlers" to reduce the thermal conductivity as well as to maintain high electrical conductivity; and consequently improve thermoelectric properties [35,57].

Apart from modification on the molecular level as described above, low thermal conductivity may also be achieved through processes such as mechanical alloying to produce nanocomposites. First proposed in the late 1950s, mechanical alloying or high energy ball milling is an established process used to achieve synthesis of nanocrystalline thermoelectric materials [58,59] through reduction of the grain size of powder particles. The enhancement in thermoelectric properties of these nanocrystalline materials is largely due to reduction of the lattice thermal conductivity, with its K_L being less than half that of comparable bulk material at room temperature [60]. The reduced lattice thermal conductivity coupled with only a slightly reduced carrier mobility yields an increase in overall ZT of these nanocrystalline materials [59].

For $Mg_2Si_{1-x}Sn_x$ thermoelectric materials, their high atomic weight, high electrical conductivity and very low lattice thermal conductivity result in a relatively high dimensionless thermoelectric figure of merit [61]. Generally, the thermal conductivity of the Mg_2Si–Sn group is in the range of 1.75–2.3 W/m K [62]. The thermal conductivity of Mg_2Si n-type at room temperature is 11.17 W/m K [63], and for the $Mg_2Si_{0.4}Sn_{0.6}$ solid solution the thermal conductivity is further reduced to about 2.1 W/m K at $T=662$ K [64]. There are several approaches to reduce the thermal conductivity for the Mg_2(Si–Sn) group, such as choosing a suitable dopant and appropriate processing technique. Zhang et al. [62] studied Mg_2(Si, Sn) composite thermoelectric materials, the results showed that the thermal conductivity of the undoped sample was 2.3 W/m K at room temperature and decreased to a minimum value of 1.75 W/m K at ~520 K. A maximum dimensionless figure of merit 0.81 at 810 K was attained for this compound. In 2011, studies were conducted by Liu et al. [40] on
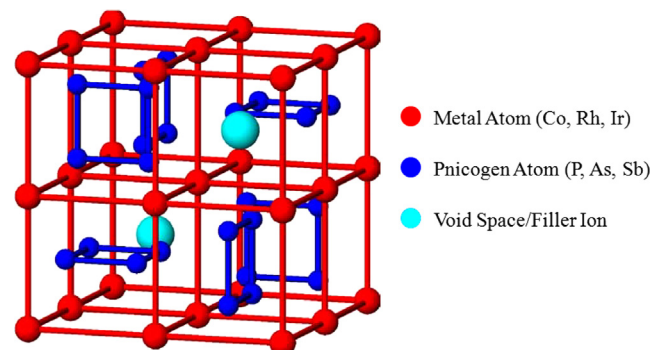

● Metal Atom (Co, Rh, Ir)

● Pnicogen Atom (P, As, Sb)

● Void Space/Filler Ion

Fig. 3. Crystal structure of filled skutterudite [35,57].

the $Mg_2Si_{0.3}Sn_{0.7}$ based material doped with Sb. The results show that Sb dopant is able to significantly reduce the lattice thermal conductivity (K_L) through increased point defect scattering. This compound is able to achieve a maximum value of $ZT = 1.0$ at 640 K. In the following year, Du et al. [65] studied $Mg_2Si_{0.5}Sn_{0.5-x}GaSb_x$; the results showed that the lattice thermal conductivity decreased with increasing GaSb dopant and a maximum dimensionless figure of merit 0.47 was obtained at 660 K.

Most of the recent investigations have been focused on solid solutions of $Mg_2Si_{1-x}Ge_x$, $Mg_2Si_{1-x}Sn_x$ and $Mg_2Sn_{1-x}Ge_x$ thermoelectric materials with the objective of simultaneously increasing the electrical conductivity while decreasing the thermal conductivity. Fig. 4 shows the variation of lattice thermal conductivity of these compositions [66].The thermal conductivity and the electrical conductivity are coupled, based on the Wiedemann–Franz law where the electronic thermal conductivity, K_e, can be estimated by the given equation [67]:

$$K_e = L_o \sigma T \qquad (6)$$

where L_o is the Lorenz number, σ is the electrical conductivity and T is the absolute temperature. The Lorentz number can be described by the following equation [68]:

$$L_o = L = (\pi K_B)^2/(3e^2) = 2.44 \times 10^{-8} \; V^2 \; K^{-2} \qquad (7)$$

where K_B is Boltzmann's constant and e is the electron charge and L is the Sommerfeld value. The Lorenz number for the $Mg_2Si_{1-x}Sn_x$ solid solutions have been found to be $1.8–1.9 \times 10^{-8} \; V^2 \; K^{-2}$ for the carrier concentration of $10^{20} \; cm^{-3}$ [69]. Therefore, the Lorenz number depends on the majority and minority carrier concentrations, as well as the temperature [45].

It was found that bulk polycrystalline compounds show a high figure of merit for n-type materials doped with Bi or Sb. It appeared that p-type materials are quite difficult to be stabilized in these phases. However, Noda et al. [70] have achieved p-type $Mg_2Si_{0.6}Ge_{0.4}$ doped with Ag, a resulting ZT as large as 1.68 at 629 K was obtained. Fig. 5 shows plots of the ZT region of material parameters of lattice thermal conductivity and weight mobility that can lead to $ZT > 1$ [71].

This discussion indicates that a good thermoelectric material must have good carrier mobility, high effective mass, and a low lattice thermal conductivity. Moreover, materials with complex crystalline structure and high atomic weight materials such as clathrates and chalcogenides are preferable for better thermoelectric materials because of their higher ability to enhance phonon scattering. However, Jeng et al. [72] conducted a comparison of the thermal conductivity between periodic and random
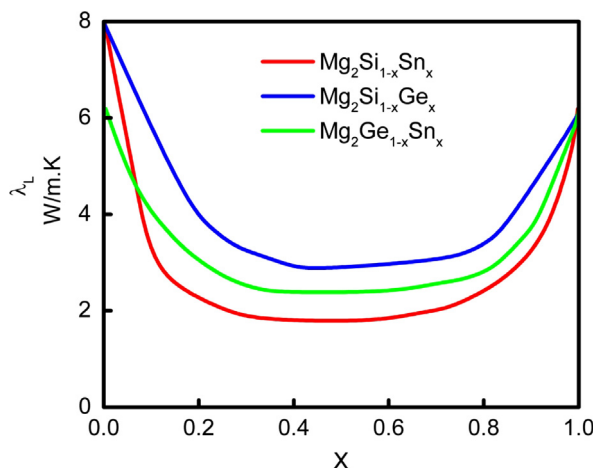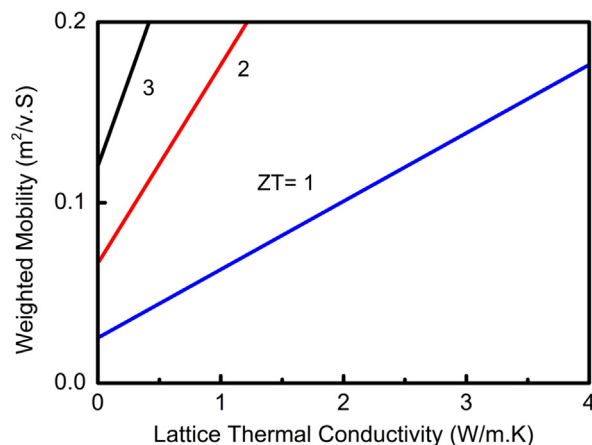

Fig. 5. Plots of constant ZT showing the region of material parameters space that can lead to $ZT > 1$. The lines are for an extrinsic, optimally doped semiconductor at room temperature, with carriers scattered by acoustic phonons [71].

nanocomposites and concluded that the randomness either in particle size or location distribution causes only slight fluctuation but is not a dominant factor for thermal conductivity reduction. The microstructural study of the high ZT material $Mg_2Si_{0.4-x}Sn_{0.6}Sb_x$ alloys showed that the lattice thermal conductivity of these materials are in the range of 1.5–2.1 W/m K at 300 K, as compared to 7.9 W/m K of Mg_2Si and 5.9 W/m K of Mg_2Sn. Interestingly, these materials showed naturally formed nanoscale compositional/structural modulations which are believed to be responsible for the low value of thermal conductivity [58]. Zaitsev et al. [73] introduced Mg_2Si and Mg_2Sn solid solutions, and the results indicated reduction in thermal conductivity and enhanced short wave-length phonon scattering, due to the presence of point defects and optimized band structure, such as band inversion and splitting.

Further investigations by Zhang et al. [74] on $Mg_2(Si–Sn)$ compounds indicated that a significant reduction of thermal conductivity from 2.2 to 1.3 W/m K at 780 K was achieved, resulting in a maximum value of $ZT = 1.1$ at 773 K for the single-phase $Mg_2Si_{0.4-x}Sn_{0.6}Sb_x$. Another study by Zhu et al. [75] on $Mg_2(Si–Sn)$ reveals that the Sb dopant and nanoscale microstructure significantly reduced the lattice thermal conductivity to less than 2.5 W/m K and thus a maximum ZT of about 1.1 at 770 K was attained. A study was also carried out by Liu et al. [41] on $Mg_2Si_{1-x}Sn_x$ based materials. The results indicated that Sn-rich precipitates of in the range of several tens of nanometers were dispersed in the $Mg_2Si_{0.4}Sn_{0.6}$ matrix. This microstructure may serve to enhance the boundary scattering of phonons, thus low lattice thermal conductivity could be achieved in the range of 300–700 K. Consequently, a maximum value of ZT of about 1.3 at 740 K was attained. In addition, a greater fundamental understanding on the physical explanation behind the reduction of lattice thermal conductivity of $Mg_2(Si–Sn)$ thermoelectric material is needed, which may contribute towards improvement of the material properties and scattering of phonons.

2.2. The Seebeck coefficient and Peltier coefficient

The Seebeck coefficient S or thermoelectric power is an intrinsic property of the material which is related to the material's electronic structure [76]. In 1821, Thomas Johann Seebeck discovered the phenomenon of thermoelectric effect, when two dissimilar materials (iron and copper) were connected together and the junctions were held at different temperatures, the voltage potential generated was proportional to the temperature difference [50]. The voltage difference is called Seebeck voltage, which

Fig. 4. Schematic plot of lattice conductivity at room temperature against concentration of second component in $Mg_2(Si,Ge,Sn)$ alloys [66].

is relative to the temperature difference between the two junctions. The Seebeck coefficient can be expressed by the following equation [59]:

$$S = V/(T_h - T_c) \tag{8}$$

where S is the Seebeck coefficient (V/K or μV/K), V is the voltage, and T_h and T_c are the temperatures of hot and cold sides, respectively. The sign of Seebeck coefficient S can be positive or negative, which indicates on the direction of the potential voltage. For p-type semiconductors, the sign of the Seebeck coefficient is positive when electricity is carried by holes. Inversely, for n-type semiconductors the sign of the Seebeck coefficient is negative when electricity is carried by electrons [77]. Moreover, the Seebeck coefficient is very low for metals and much larger for semiconductors [35]. Studies were conducted by Du et al. [78] on $Mg_2Si_{0.4}Sn_{0.6}$ doped with Sb. The results show improvement on the carrier concentration, electronic effective mass and electrical conductivity, but decrease of the Seebeck coefficient from -247.6 μV/K to -87.8 μV/K, because of increase of the Mg excess content. The dimensionless figure of merit of about 0.85 was achieved at 700 K for this compound. Isoda et al. [79] studied $Mg_2Si_{0.4}Sn_{0.6}$ doped by Bi, and found that the Seebeck coefficient decreased from -461.7 μV/K at 435 K of undoping to -263.7 μV/K at 815 K with Bi-doping. A maximum ZT of 0.87 was attained at 630 K. Another study was conducted by You et al. [80] on $Mg_2Si_{0.4}Sn_{0.6}$ thermoelectric material doped by Sb. The result shows enhancement of the Seebeck coefficient about -300 μV/K. The maximum figure of merit of 0.64 was achieved at 723 K for $Mg_{2.2}Si_{0.7}Sn_{0.3}Sb_{0.01}$. A further study by Liu et al. [61] on Mg_2Si and Mg_2Sn doped with Sb indicated that the Seebeck coefficient progressively increased and the thermoelectric figure of merit ZT reached exceptionally large values, approximately 1.3 near 700 K.

On the other hand, the phenomenon of the Peltier effect which was discovered by Peltier in 1834 observed that when an electrical current is applied to the junctions of two dissimilar materials, heat is either absorbed or liberated (carried by electrons or holes) at the junctions depending on the direction of the current, one junction becomes hot and the other becomes cold. The Peltier effect can be calculated by the following formula [59]:

$$\Pi = Q/I \tag{9}$$

where Π is the Peltier coefficient, Q is the amount of heat and I is the electrical current. Indeed, the Peltier coefficient and the Seebeck coefficient can be expressed in the Kelvin relations by the following formula [15]:

$$\Pi = S \cdot T \tag{10}$$

Studies conducted by Nolas et al. [81] mentioned that the relation between the Seebeck voltage and the temperature is linear only for small changes in temperature. However, for high temperature ranges the relationship becomes non-linear. It is therefore important to state the temperature at which the Seebeck coefficient is being specified. Nevertheless, Tirtt et al. [82] suggested that a thermopower > 225 is required to achieve $ZT > 2$.

2.3. The power factor

The power factor is defined as the ability of a material to produce useful electrical power. It has been found convenient to introduce a quantity known as the power factor that contains both the Seebeck coefficient S and the electrical conductivity σ, as an indication of the power produced by the thermoelectric material. The classical approach to achieve a high value of the power factor with high Seebeck coefficient S and electrical resistivity ρ or $(1/\sigma)$

can be represented by the following equation [60]:

$$PF = S^2/\rho \tag{11}$$

The optimization of the thermoelectric material properties by enhancement of the power factor (high electrical conductivity) and reduction of the thermal conductivity K_{ph} was conceived by Slack through introduction of the concept of phonon–glass–electron–crystal (PGEC) materials [35,37]. The PGEC describes an ideal thermoelectric material that should have a low lattice thermal conductivity as in a glass or an amorphous material, and a high electrical conductivity as in a crystal, such as skutterudites ($CoSb_3$), clathrates ($Ba_8Ga_{16}Ge_{30}$) and Zintl phases [75]. Slack estimated that an optimized PGEC material would have values of $ZT = 4$ in the 77–300 K temperature range [107]. The PGEC approach is a superior strategy which can reduce the thermal conductivity without affecting electronic properties, which subsequently enhances ZT of the thermoelectric material. In recent years, PGEC materials have significantly contributed to improve the field of thermoelectric primarily through the reduction of lattice thermal conductivity [61,75].

The carrier concentration that yields the maximum power factor of a given material is usually close to that which gives the highest figure of merit [66]. Generally, the range of electrical resistivity for semiconductor materials lies between 10^3 and 10^{-8} S/cm [83]. The electrical conductivity of Mg_2Si n-type at room temperature is 56.8 S/cm and possesses a carrier concentration of 2.24×10^{18} cm^{-3} at room temperature [63]. For example, in 2012, Du et al. [65] investigated the $Mg_2Si_{0.5}Sn_{0.5-x}GaSb_x$ solid solutions prepared by the B_2O_3 flux method followed by hot pressing. The results showed that the electrical conductivity increased to about 14.9×10^3 S/m while the lattice thermal conductivity decreased (2 W/m K) with increasing GaSb content about 0.08. The maximum dimensionless figure of merit of about 0.47 was obtained at 660 K. In the same year, Du et al. [84] further studied $Mg_2Si_{0.58}Sn_{0.42-x}Bi_x$ n-type thermoelectric materials. The results showed that the electrical conductivities increased to $\sim 35 \times 10^3$ S/m with the increase of Bi doping, while enhancement of the power factor resulted in a maximum value of the dimensionless figure of merit of 0.65 at 700 K. Another study was carried out by Zhang et al. [62] on Mg_2Si and Mg_2Sn doped with La, where the Mg_2Si-rich bulk grains were in situ coated by Mg_2Sn-rich thin layers. It was found that the La doping dramatically increased the ratio of electrical conductivity to thermal conductivity to $\sim 2.5 \times 10^4$ V^2 K in the composites which concurrently improved the power factor. As a result, a dimensionless figure of merit, $ZT = 0.81$, was attained at 810 K for $Mg_{2-x}La_x(Si,Sn)$. Recent studies were conducted by Gao et al. [45] on $Mg_2Si_{0.5-x}Sn_{0.5}Sb_x$, which was synthesized by a facile and cost-effective B_2O_3 flux method in air. The results showed that a peak power factor of 3.2×10^{-3} W/m K^2 was achieved at 610 K, and obtained the maximum $ZT \sim 0.9$ at 780 K. A maximum power factor of Sb-doped Mg_2Si of about 3.0×10^{-5} W/cm K^2 at 773 K was achieved by Kajikawa et al., and 3.3×10^{-5} W/cm K^2 at about 650 K was achieved by Zhang et al. which indicated significant power improvement of the Mg_2Si–Sn group as one of the leading candidates for materials in thermoelectric applications [85]. Research was conducted by Liu et al. [40] on $Mg_2(Si_{0.3}Sn_{0.7})_{1-x}Sb_x$ thermoelectric materials fabricated by solid-state reaction and spark plasma sintering. The results showed that high electrical conductivity and Seebeck coefficient can be obtained, corresponding to a high power factor in the range of 3.45–3.69 mW/m K^2 in the temperature range of 300–660 K, and reached a maximum $ZT = 1.0$ at 640 K. Liu et al. have performed studies on $Mg_2Si_{1-x}Sn_x$ solid solution doped by Sb, which showed enhancement of the power factor and improvement of the dimensionless figure of merit. The highest ZT reached 1.11 at 860 K [86] and 1.25 at 800 K [87].

Evident improvement in the electrical conductivity is the main driver in the improved performance of $Mg_2(Si–Sn)$ solid solution as thermoelectric materials. Accordingly, large effective masses can yield high power factor, a similar effect with low thermal conductivity may achieve very high values of ZT. However, the theoretical and experimental studies confirmed that significant improvement on power factor can be achieved to enhance ZT.

3. Electronic properties

3.1. Scattering mechanism for carriers

In solids, an important transport behavior is the scattering which is caused by carriers or phonons. The carrier scattering directly affects the electrical conductivity and the Seebeck coefficient, whereas phonon scattering affects the thermal conductivity [51]. Therefore, the transport properties of a semiconductor depend strongly on scattering mechanisms such as acoustical phonon and optical phonon scatterings, ionized impurity scattering, and neutral impurity scattering. When the external forces are applied to the semiconductor, the charged carriers will reach the steady-state conditions by the above-mentioned scattering mechanisms, and will eventually return to equilibrium conditions when these forces are removed from the semiconductor [77].

In the semiconductor carrier-phonon scattering process, there are many possibilities that a carrier can undergo a change in state, the availability of states, absorbing probability or phonon emitting, and the carrier phonon interaction strength. Stationary defects such as impurities and dislocations and the dynamic defects such as electrons, holes, and lattice phonons have a high possibility to scatter the charge carriers in a semiconductor. Therefore, the types of scattering mechanisms involved will determine the overall transport properties of a semiconductor [77]. Furthermore, complex structures and high average atomic weight materials are preferable for improving the thermoelectric materials through enhancement of phonon scattering and thus reducing the thermal conductivity.

3.2. Carrier concentration

Generally, in intrinsic semiconductor materials, there are two common types of charge carriers, either electrons or holes. The interrelationship between carrier concentration and Seebeck coefficient for degenerate semiconductors can be expressed by the following equation [88]:

$$S = (8\Pi^2 K_B^2 / 3eh^2) \times m \times T \times (\Pi/3n)^{\wedge 2/3} \tag{12}$$

where n is the carrier concentration and m^* is the effective mass of the carrier. An increase in the effective mass can yield very high Seebeck coefficients, thus increasing the power factor and ultimately enhance ZT. Fig. 6 reveals the maximum efficiency (ZT) of thermoelectric with a variation of σ, S, K as a function of carrier concentration (n) [35,88,89]. This implies that an increase in carrier concentration not only increases electrical conductivity but also increases thermal conductivity and decreases the Seebeck coefficient. Moreover, the thermoelectric power factor $PF = S^2 \cdot \sigma$ reaches a maximum at higher carrier concentration than ZT. The difference between the peak in $S^2 \cdot \sigma$ and ZT is greater for the newer lower K_L materials. The reduction of lattice thermal conductivity K_L can offer to a two-fold benefit for the thermoelectric figure of merit, which leads to a larger Seebeck coefficient and allows to reoptimize the carrier concentration [88]. The carrier concentration, through measurement of the Hall effect, may be
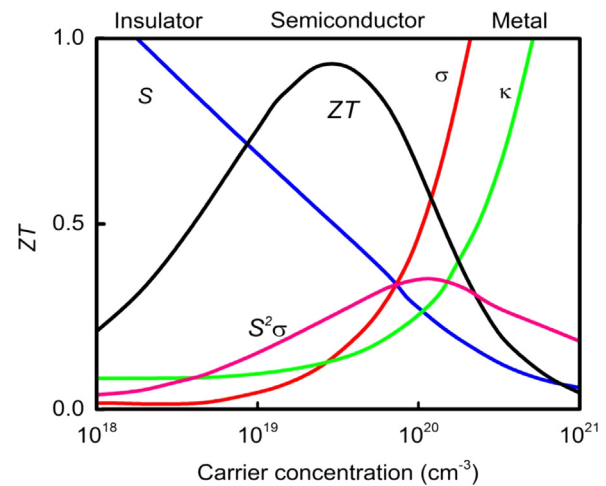

Fig. 6. Comparison of thermoelectric parameters: Seebeck coefficient, electrical conductivity, thermal conductivity and figure of merit [35,88,89].

determined from the following relationship [78]:

$$R_H = 1/n \cdot e \tag{13}$$

where R_H is the Hall coefficient and e is the electronic charge. Thus, carrier concentration (n) and the carrier mobility (μ) are related to the electrical conductivity (σ) can be defined as [88]

$$\sigma = ne\mu \tag{14}$$

where μ is the electron mobility which may be defined in terms of the conductivity σ, effective mass m_c^* and the relaxation time τ, by the following formula [77]:

$$\mu = q(\tau) / m_c^* \tag{15}$$

Eq. (2) clearly shows that a good thermoelectric material must possess high carrier mobility ($\sim 1000\ cm^2/V\ s$ for Bi_2Te_3 and skutterudites) [76], high effective mass, and low lattice thermal conductivity, which lead to the formulation of the concept of "phonon–glass–electron–crystal" as discussed previously. This typically occurs in heavily doped semiconductors with optimum carrier concentrations between 10^{19} and 10^{21} carriers per cm^3, which falls in between common metals and semiconductors [90].

The coupling between all the thermoelectric parameters σ, S, and K makes the improvement of ZT difficult. Heavily doped semiconductors are useful for modulating thermoelectric performance. Changes in the dopant and doping concentration in semiconductors may affect corresponding changes in electrical conductivities and carrier type without much affecting other properties [51]. For example, doped semiconductor materials may achieve a higher electrical conductivity ($\sim 10^5$ S/m) and remarkably higher Seebeck coefficient ($\sim 200\ \mu V/K$), while the thermal conductivity remains relatively insignificant (~ 0.5 W/m K) [51]. In 2011, Gao et al. [48] studied the Mg_2 (Si–Sn) Sb-doped thermoelectric material. It was found that the carrier concentration increased with the Sb content, thus an improvement of the power factor and thermoelectric figure of merit was achieved. In the following year, Liu et al. [41] investigated the $Mg_2Si_{1-x}Sn_x$ based compounds, which showed enhancement on the carrier concentration from 2.28×10^{18} for the undoped compound, to 2.36×10^{20} for doping compounds. These materials possessed excellent thermoelectric properties and achieved a high value of ZT. Du et al. [84] studied n-type $Mg_2Si_{0.58}Sn_{0.42-x}Bi_x$. The results showed that the carrier concentrations increased with the increasing Bi-doping and reached the maximum dimensionless figure of merit of 0.65. A study was conducted by Isoda et al. [79] on $Mg_2Si_{1-x}Sn_x$ of the Bi-doped

thermoelectric material. The results demonstrated that when the carrier component of thermal conductivity was increased, the phonon component of thermal conductivity was decreased slightly. The dimensionless figure of merit showed noticeable enhancement of the maximum value of $ZT=0.87$ at 630 K using a single-phase of $Mg_2Si_{0.5}Sn_{0.5}$.

Another study carried by Zhang et al. [62] on Mg_2(Si, Sn) with La doping showed that the carrier concentration for the doped samples is in the range $4-9 \times 10^{19}$ cm^{-3}, compared with 4×10^{18} cm^{-3} of the undoped sample, and correspondingly demonstrated enhancement in ZT of the doped composite. Research conducted by Tani and Kido [85] on Mg_2Si showed that the carrier concentration of non-doped Mg_2Si is 4.3×10^{17} cm^{-3}, while the carrier concentration increased with Sb-doped compounds in the range of $0.22-1.5 \times 10^{20}$ cm^{-3}, which also correspondingly increased the thermoelectric performance. A further study by Gao et al. [45] on $Mg_2Si_{0.5-x}Sn_{0.5}Sb_x$ thermoelectric materials showed that the carrier concentration was about 4.9×10^{16} cm^{-3} for the undoped compound, and was substantially increased to $3.3-7.1 \times 10^{20}$ cm^{-3} for the doped compound, due to the effective electron doping by Sb. Carrier concentration was found to be increased with an increasing dopant value, and while the carrier mobility roughly decreased due to the enhancement of carrier–carrier scattering. The maximum ZT values of >0.9 were reproducibly obtained at 780 K. In addition, Du et al. [84] studied $Mg_2Si_{0.58}Sn_{0.42}$ composites with Bi additive and found that the carrier concentration was considerably increased from 1.8×10^{18} of the undoped samples, $0.27-1.2 \times 10^{20}$ cm^{-3} for the doped samples.

Furthermore, there is a strong correlation between the Mg excess content and the carrier concentration: where the carrier concentrations for $Mg_2Si_{0.5}Sn_{0.5}$ doped with 1.5 mol% Sb are 3.9×10^{20} cm^{-3} and 2.5×10^{20} cm^{-3} for a nominal Mg excess of 10 mol% and 5 mol%, respectively [78]. Therefore, a literature of $Mg_2Si_{1-x}Sn_x$ thermoelectric based material shows that the carrier concentration was significantly increased with a heavy dopant, while the electronic properties have been improved and enhanced the dimensionless figure of merit to yield a peak value.

3.3. Band gaps of $Mg_2Si_{1-x}Sn_x$ thermoelectric materials

The band gap or energy gap is the difference in energy levels of a solid material where electron states can exist [35]. The band gap generally refers to the energy difference between the top of the valence band and the bottom of the conduction band in insulators and semiconductors. The band gap is a major factor in determining the electrical conductivity of a solid, where substances with large band gaps are generally insulators and those with smaller band gaps are called semiconductors, while conductors either have very small band gaps or none, due to the overlap in the valence and conduction bands [35,91]. When the valence electrons are excited into the conduction band, the conductivity of a semiconductor increases. The energy gap for most semiconductors may vary between 0.1 and 6.2 eV [77]. However, decreased band gap semiconductors, which can induce an exponential increase in charge carrier concentrations, are considered most desirable [92]. Theoretical studies of the electronic structure of Mg_2Si-Sn compounds have been carried out by several groups using the pseudopotential method, they were found to be anti-fluorite type structures of small band gap with indirect band gaps of 0.51 eV for $Mg_2Si_{0.6}Sn_{0.4}$, 0.77 eV for Mg_2Si, and 0.35 eV for Mg_2Sn [93]. Furthermore, $Mg_2Si_{0.3}Sn_{0.7}$ was found to possess a smaller band gap compared to $Mg_2Si_{0.4}Sn_{0.6}$ and $Mg_2Si_{0.5}Sn_{0.5}$, which is promising for obtaining higher electrical conductivity [40]. As a comparison, band gaps for well-known semiconductors are 1.12 eV for silicon (Si), 0.7 eV for germanium (Ge) and 0.08 eV for tin (Sn) [51,77,94].

In addition, for the two compositions $Mg_2Si_{0.4}Sn_{0.6}$ and $Mg_2Si_{0.5}Sn_{0.5}$, the band gaps are about ~ 0.1 eV, and then increased

to 0.25 eV for compositions richer in Mg_2Si [95], and for Mg_2Si_{1-x} Ge_x solid solutions the band gap is between 0.05 and 0.23 eV [77,96]. Theoretically, the band gap of the semiconductor Mg_2Si was found to be 0.2–0.7 eV, while Mg_2Sn was determined to be a bad metal with a density of states at the Fermi level of 0.3 states eV^{-1} [97]. This prediction was confirmed experimentally to yield an energy band gap of 0.75–0.8 eV for Mg_2Si [63], 0.7–0.75 eV for Mg_2Ge and 0.3–0.4 eV for Mg_2Sn [96]. In 2011, Lee et al. [98] studied Mg_2Si based materials. The results showed that the band gap remained unchanged at about 0.77 eV, although the electrical conductivity was consequently increased at high temperatures. Liu et al. [99] indicated that the variations of Ga doping amount as well as the Mg content do not affect the band gap value of $Mg_{2(1+z)}(Si_{0.3}Sn_{0.7})_{1-y}Ga_y$, which remained at about $E_g=0.49-0.50$ eV for all the samples. Research conducted by Gao et al. [48] on $Mg_2Si_{0.7}Sn_{0.3}$ showed that the band gap of Sb-doped samples varied little with the amount of the Sb dopant as compared with the undoped samples. The trivial changes in E_g suggest that doping with Sb atoms has only a minor effect on the band gap of $Mg_2Si_{0.7}Sn_{0.3}$ around 0.37–0.38 eV. Nevertheless, the band gap of the Mg_2Si–Sn group showed slight changes while doping with elements or almost unchanged. Thus, the important role is played not only by the band gap width but also by the energy gap between the subbands [100]. Two subbands of the conduction band are separated by a small gap ($\Delta E < 0.5$ eV), and they have been created from states of Mg and of the element of the IV-group. In the $Mg_2Si_{0.4}Sn_{0.6}$ solid solution the gap between subbands is practically equal to zero. In this case the electrons of both subbands take part in the transport phenomena, which results in an increase in the thermoelectric figure of merit [101].

4. Mg₂(Si–Sn) thermoelectric materials

Mg_2(Si–Sn)-based solid solutions have attracted a great deal of attention because of their widely available base materials, environment-friendly constituent elements, and promising thermoelectric performance with higher figure of merit for the mid-temperature range [102–109]. The power output per unit mass of many known thermoelectric materials can be lower than the Mg_2(Si–Sn) thermoelectric material. For example, the density of Bi_2Te_3 (7.93 g/cm^3), PbTe (8.27 g/cm^3), $CoSb_3$ (7.625 g/cm^3), and $Si_{0.8}Ge_{0.2}$ (2.93 g/cm^3) are significantly higher than $Mg_2Si_{0.4}Sn_{0.6}$ which is only 2.9 g/cm^3 [45]. Fig. 7 illustrates the current thermoelectric materials and indicates that Mg_2(Si–Sn) based materials are promising thermoelectric materials with high ZT [33]. The mobility of holes for $Mg_2Si_{0.4}Sn_{0.6}$ solid solutions is smaller than
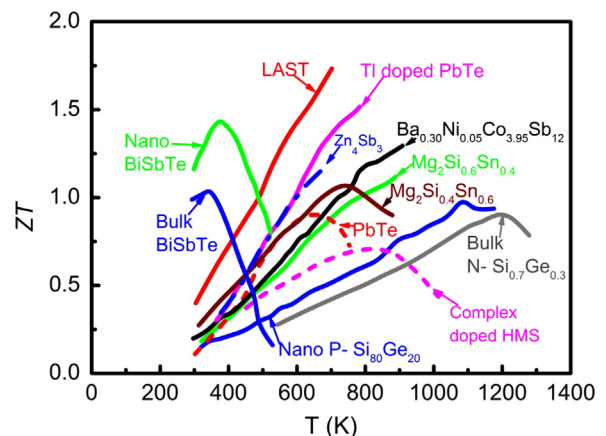

Fig. 7. State-of-the-art comparison of ZT in conventional bulk materials and nanostructured composite materials [33].

that of electrons by a factor of 2 [108]. The thermoelectric properties of the compounds Mg_2Si and Mg_2Sn, together with their solid solutions, have been mostly interesting because of the significant decrease in the thermal conductivity compared with the pure compounds [66]. Although the figure of merit ZT of undoped $Mg_2(Si–Sn)$ based materials is small, about 0.18 at 540 K [62], there is a great opportunity to improve the $Mg_2(Si–Sn)$ thermoelectric material through a suitable technique for medium temperature applications. Nevertheless, several investigations have been carried out regarding electrical, optical, and thermal properties of $Mg_2(Si–Sn)$ [110–112].

The $Mg_2(Si–Sn)$ based material is abundant in the earth's crust, silicon has the second highest Clarke number and magnesium has the eighth highest [113]. Correspondingly, the low cost of these elements as thermoelectric materials is implied, thus attracting considerable interest as prospective thermoelectric materials in the medium temperature range [114,115]. The Clarke number is expressed as the average content of the chemical elements in the earth's crust. Magnesium silicide belongs to the family of magnesium (IV) group that crystallizes in the anti-fluorite structure phase with Si in face-centered cubic positions and Mg in tetrahedral sites, and with three atoms per primitive unit cell, and the Fm-3m space group fixes the fractional coordinates of all atoms. The molecular structure of Mg_2Si is shown in Fig. 8 [46,69].

Until now, the most tried approach to improve the thermoelectric performance of the $Mg_2(Si–Sn)$ based material has been the tuning of the electrical and thermal properties by the grain size and doping or substitution elements. Fig. 9 demonstrates the main thermoelectric properties of n-type $Mg_2Si_{0.4}Sn_{0.6}$ solid solution [101]. The best results of ZT were reported for $Mg_2Si_{0.6}Sn_{0.4}$ based thermoelectric materials rising from just over 0.4 at 500 K [66] to 1.3 at 740 K [41]. Thus, development of thermoelectric materials with higher efficiency is one of the main current interests in the research of thermoelectric materials. Table 1 shows the comparison of properties of mechanically alloyed $Mg_2Si_{1−x}Sn_x$ thermoelectric compositions [41,48,79,80,116]. Fig. 10 shows two different phase diagrams for the $Mg_2Sn–Mg_2Si$ quasi-binary system [116]. In addition, there is significant potential to enhance $Mg_2(Si–Sn)$ thermoelectric materials through which various methods are expected to be achieved.

5. Improvement of $Mg_2Si_{1−x}Sn_x$ thermoelectric materials through fabrication techniques

Several different compaction techniques have been utilized to synthesize thermoelectric materials. The fundamental principle behind most of the techniques is to apply high pressure for densification, and frequently a relatively high temperature to soften the materials, to allow better filling and material flow by diffusion to eliminate the remaining porosity. The challenge is to achieve very high density close to the theoretical density and low porosity without losing the nanoscale microstructure and retaining the chemical purity of the material. There are several methods that can be used to consolidate thermoelectric materials such as mechanical alloying, microwave irradiation [34], field-activated and pressure-assisted synthesis (FAPAS), hot pressing (HP) and spark plasma sintering (SPS) [85,117].

Hot pressing is a favored technology used for powder consolidation and manufacturing processes of high performance thermoelectric materials. Hot pressing technology is mainly used to fabricate powder materials, through application of high pressure (80 MPa) with high temperature (900–1073 K) to the

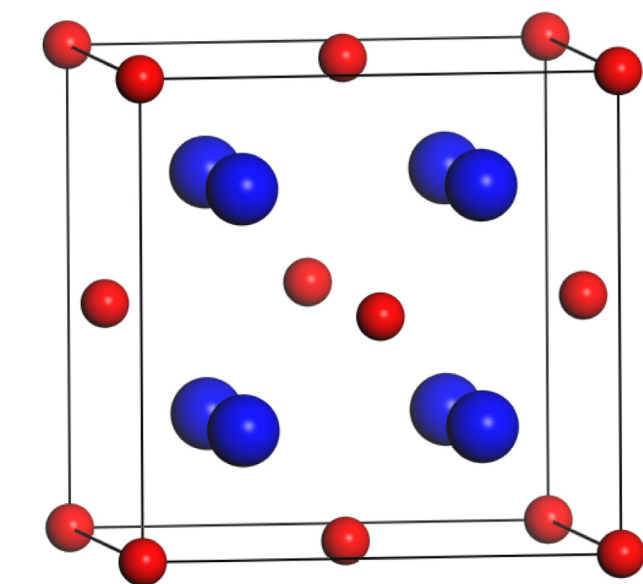**Fig. 8.** (a) Unit cell of Mg_2Si anti-fluorite structure with the Fm3m space group; Mg atoms (large blue circles) and Si atoms (small red circles) [46,69]. (For interpretation of the references to color in this figure caption, the reader is referred to the web version of this paper.)
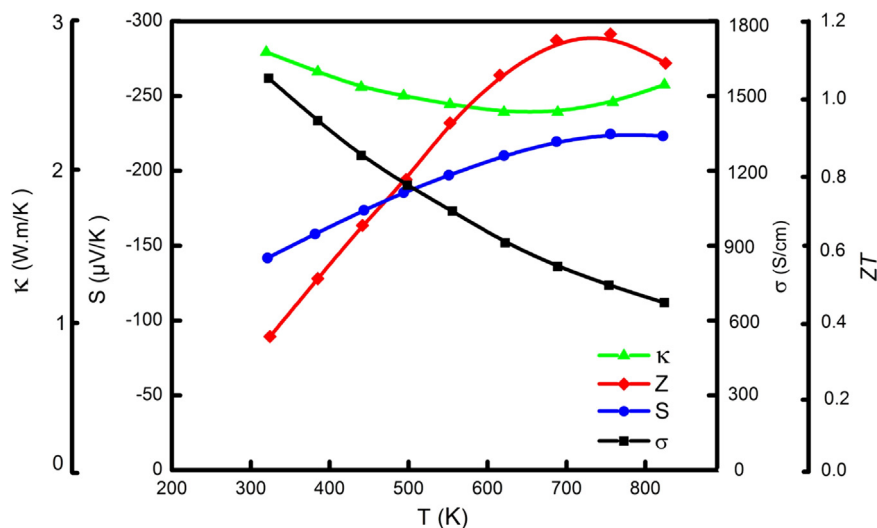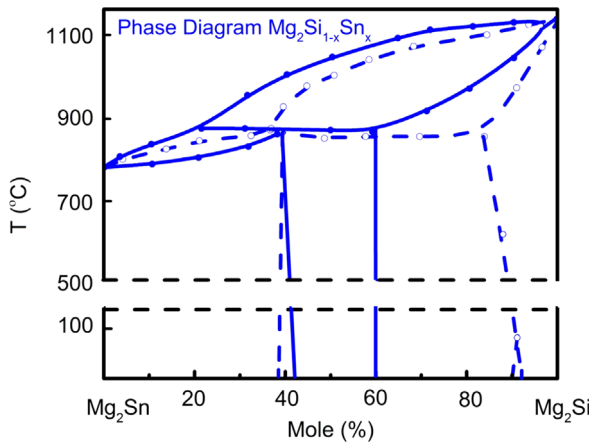

Fig. 9. Thermoelectric properties of n-type $Mg_2Si_{0.4}Sn_{0.6}$ solid solution [101].

Table 1
Comparison properties of mechanically alloyed $Mg_2Si_{1-x}Sn_x$ compositions at different temperatures [41,48,79,80,116].

Properties	Mg_2Si	$Mg_2Si_{0.8}Sn_{0.2}$	$Mg_2Si_{0.6}Sn_{0.4}$	$Mg_2Si_{0.7-x}Sn_{0.3}Sb_x$	$Mg_2Si_{0.5}Sn_{0.5}-Bi$	$Mg_{2.2}Si_{0.7}Sn_{0.3}Sb_{0.01}$	$Mg_{2.16}(Si_{0.6}Sn_{0.4})_{0.985}Sb_{0.015}$
ρ (g/cm³)	1.94	2.35	2.85	N/A	N/A	N/A	N/A
σ (1/Ω cm)	0.11	600	450	N/A	6.56×10^{-6}	N/A	N/A
n (1/cm³)	3×10^{16}	3×10^{20}	3×10^{20}	$1.89-9.29 \times 10^{19}$	1.9×10^{26}	1.8×10^{19}	1.67×10^{20}
μ (cm²/V s)	21	18	20	19.88–29.02	N/A	1.74×10^{-1}	56
K (W/m K)	5.3	3.9	2.6	3.6–2.4	1.93–2.61	1.37	0.5
K_{ph} (W/m K)	5.3	3.4	2.3	N/A	1.75–1.91	N/A	N/A
μ/K (cm²K/V J)	400	530	870	N/A	N/A	N/A	N/A
S (μV/K)	−620	−65	−90	N/A	103.34	−270	N/A
T (K)	300	300	300	620	630	723	740
ZT	4.4×10^{-4}	0.023	0.03	0.55	0.87	0.64	1.3

Fig. 10. Two different phase diagrams for the Mg_2Sn-Mg_2Si quasi-binary system [116].

Fig. 11. Spark plasma sintering technology [121].

specimen simultaneously [74,75]. Preparing homogeneous thermoelectric materials is crucial by extended time of annealing of the hot pressing method. In addition, this method offers the opportunity to (a) improve mechanical properties, (b) enhance thermoelectric properties of material, and (c) significantly simplify production engineering of thermoelements [118]. Studies were conducted by Isoda et al. [119] on p-type $Mg_2Si_{0.25}Sn_{0.75}$ with Li and Ag double doping using the liquid solid reaction method and hot pressing. The results showed an improvement in thermoelectric properties and increase in the carrier concentration (4.12×10^{25} m^{-3}) with the double doping, where the figure of merit reached 0.32 at 610 K.

Gao et al. [48] investigated Sb-doped $Mg_2(Si-Sn)$ thermoelectric materials, which were fabricated using three different processes: induction melting, solid-state reaction, and a hot press sintering technique. The results found that the carrier concentration increased with an increase in the Sb content. Sb doping has shown an improvement in the power factor and thermoelectric figure of merit ZT of 0.55 at 620 K. Studies were conducted by Isoda et al. [79] on $Mg_2Si_{1-x}Sn_x$ of the Bi-doped semiconductor, using a liquid–solid reaction followed by the hot pressing method. The results showed that the dimensionless figure of merit enhanced the maximum value of $ZT=0.87$ at 630 K with a single-phase of $Mg_2Si_{0.5}Sn_{0.5}$. In addition, hot pressing was found to be a very promising technique which can improve thermoelectric materials properties, while the Seebeck coefficient exhibited increasing trend and also showed improvement in the power factor which yielded a peak value of the thermoelectric figure of merit.

Developments in thermal technology introduced the spark plasma sintering (SPS) technology, which is also known as field
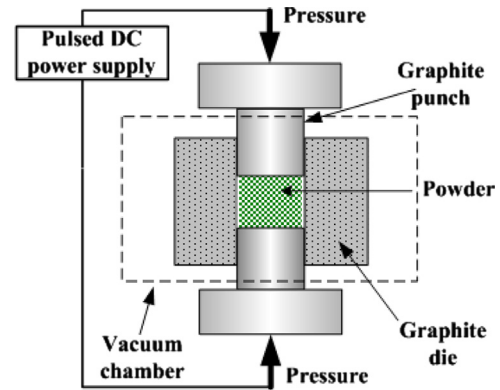
assisted sintering technique (FAST) and the pulsed electric current sintering (PECS) process. SPS is a rapid sintering technique that is assisted by pressure and electric field which consolidate powder materials [120]. The main characteristics of the SPS technique is that it utilizes high pulsed current through the graphite mould to activate the consolidation and reaction-sintering of powder materials under a low voltage [34,58], and then electrical discharges will occur. The technical parameters are high temperature, pressure and formation of good contact between the powder particles. SPS also has the additional advantage of eliminating gases and moisture which is adsorbed on the surface of the nanoparticles and arcs can defect the oxide layers. SPS has the unique advantage of using DC current to generate internal heat, as opposed to conventional hot pressing, where the heat is provided by external heating elements. The clear benefits of SPS are the ability to retain nanostructures and significant time saving (within a few minutes) and energy, while other traditional methods require hours to reach peak temperature. Densities very close to theoretical densities and excellent thermoelectric performances have been achieved by SPS processes [58]. Fig. 11 shows the stoichiometric diagram of park plasma sintering technology [121]. Furthermore, the comparison between spark plasma sintering (SPS) and hot pressing (HP) techniques is shown in Table 2 [121].

Studies carried out by Han et al. [122] on n-type $Mg_2(Si, Sn, Sb)$ as raw material alloys were prepared by an induction melting and the SPS method. The Seebeck coefficient S and electrical resistivity ρ first increased and then decreased with the increase in the amount of doping. The ZT value for $(Mg_2Si_{0.95}Sb_{0.05})_{0.4}(Mg_2Sn)_{0.6}$ reached the highest value of 1.22 at 773 K. Tani et al. [123] studied the thermoelectric properties of Al-doped $Mg_2Si_{0.9}Sn_{0.1}$ fabricated by spark plasma sintering. The results showed that the electron concentration was controlled up to 5.3×10^{19} cm^{-3} and showed a maximum value of the figure of merit ZT of 0.68 at 864 K, which is six times larger than that of the undoped specimen. A study

Table 2
Comparison of spark plasma sintering (SPS) and hot pressing (HP) techniques [121].

Parameter	SPS	HP
Heating rate	> 2000 °C/min	Limited to 80 °C/min
Productivity	Enhanced by high heating rate	Limited by long processing time
Electric power consumption	Low	< 1/3 than required for SPS
Control for the thermal gradient for functional graded materials and selective control of the density in specified regions	Enabled by punch die geometry and current distribution	Not possible
Nanosintering and sintering under meta-stable conditions	Promoted by the high heating rate and short sintering time	Grain coarsening promoted by the slow heating process

conducted by Liu et al. [41] investigated the $Mg_2Si_{1-x}Sn_x$ based compounds which were fabricated by a two step solid state reaction followed by spark plasma sintering. The results indicated that a high value of ZT could be achieved, of about 1.3 at 740 K.

Spark plasma sintering (SPS) techniques have revealed a large improvement in thermoelectric material properties compared to other techniques such as hot pressing and cold pressing. In addition, the advantages of the SPS technique include very high density and controlled porosity, combination of the compaction and sintering stages in one operation, inexpensive operation cost, rapid cycle times and minimal grain growth [121]. On the other hand, the disadvantages of spark plasma sintering are that only simple symmetrical shapes may be prepared, and an expensive pulsed DC generator is required [121].

6. Nanostructuring the grain size of $Mg_2Si_{1-x}Sn_x$ for thermoelectric potential

Traditional approaches of thermoelectric material properties were influenced by the types of dopants and their concentrations to maximize the power factor $S^2\rho$ and enhanced ZT [124]. Both theoretical and experimental research have been trying alternative approaches to develop thermoelectric materials by various distinct strategies such as exploring effective methods for phonon scattering, introducing nanostructured grain size, grain shape, secondary phases, dimension reduction and introduction of porosity to increase the performance of the bulk thermoelectric materials [125–131]. Therefore, as mentioned earlier, Hicks and Dresselhaus established the idea of nanoscale thermoelectric materials approach using reduction in dimensionality, which offer new strategies to vary S, σ, and K independently and enhance ZT [132]. For example, nanostructures such as quantum dots may cause dramatic enhancement on the density of states near to E_f, leading to improvement in the Seebeck coefficient and increased carrier mobilities, while nanocomposites and nanowires provide enhanced boundary scattering of phonons at the barrier well interfaces [133]. Furthermore, the thermal conductivity of the quantum well structures is smaller than the bulk, because the quantum well/barrier interfaces considerably enhance the phonon–phonon scattering without significantly increasing the electron scattering [134].

Given the ability of nanostructures to break through the barriers in thermoelectric material performance, development of bulk nanostructured materials for fabrication of a large-scale TEGs' application has been a key area of research [135]. Mechanisms such as energy filtering at grain boundaries and phonon scattering are strategies that have been employed to improve the thermoelectric figure of merit [136]. For example, employing nanoparticles with a wide distribution of sizes will result in phonon scattering over both long and short wavelengths, thus further reducing the thermal conductivity of the material [137]. Fig. 12 shows a classification of the improvement in the nanocomposite

morphologies in terms of parameters such as dimension reduction, size reduction of a second phase and grain refinement [138].

In particular, grain refinement is a viable strategy for achieving a higher ZT. Many nucleation sites are available during the solidification, which result in a fine grain structure which is desirable for reduced thermal conductivity. The mechanism of grain formation is defined by the rate of cooling for the material, where a rapid cooling results in smaller grain size and coarse-edged granules. The value of figure of merit obtained with small grain size materials is significantly higher than that of large grain size with the same carrier concentration. Nanostructured and fine grain sized bulk thermoelectric materials can be achieved by mechanical alloying, rapid solidification, ball milling and hot pressing [139]. The advantage of using ball milling for the synthesis of nanostructured materials has the ability to produce bulk quantities of materials at room temperature conditions in a solid state using simple equipment [126]. Planetary ball milling is a simple and cost-effective method of breaking down powder particles using mechanical impact and friction. Parameters of the ball milling process are milling time, milling speed, ball to powder weight ratio (BPR), ball size distribution, and materials of the milling container [140]. Properly executed ball milling under inert conditions will result in the formation of nanostructured materials with the significant ZT, up to 250% for both n- and p-type $Si_{1-x}Ge_x$ alloys [59].

Enhancement on of thermoelectric performance through reduction of grain sizes using nanostructuring approaches have been demonstrated by several experimental works. For example, Pshenai-Severin et al. [141] reported that the thermoelectric materials with 30 nm grain size showed an increase in ZT of about 38% compared to microsized grains. Bux et al. [59] showed that the grain sizes were reduced to 20 nm, the lattice thermal conductivity could be reduced about 90%. Also, Wang et al. [142] studied the nanostructuring approach for SiGe alloys. The result showed a significant reduction in the thermal conductivity about 2.5 W/m K, much lower than that of the conventional bulk alloys about 4.6 W/m K, and increased density of nanograin boundaries, resulting in a peak ZT of about 1.3 at 900 °C. Table 3 shows a comparison of maximum ZT values for bulk and nanostructured thermoelectric materials [135]. Satyala and Vashaee [143] studied the analysis of Mg_2Si nanostructuring, the results showed that the decrease in the grain size from 20 nm to 5 nm, led to a 36% reduction of K, and enhancement of the power factor. Another study on nanoparticles showed a significant reduction in thermal conductivity of about 50% and a 2-fold increase in ZT [144]. In the case of $Mg_2Si_{1-x}Sn_x$ solid solutions a ZT value of 1.2 for bulk crystals was achieved, which was further improved to 1.4 for bulk nanostructured materials [145]. Nanocomposite thermoelectric materials have also gained interest for large-scale commercial applications [47]. For example, in 2009, Wang and Mingo theoretically demonstrated the introduction of nanoparticles into $Mg_2Si_xGe_ySn_{1-x-y}$ alloys, which considerably improves the ZT [113]. Fig. 13 illustrates the effect of grain size through the electrical, thermal conductivities and figure of merit of Mg_2Si thermoelectric materials [143].
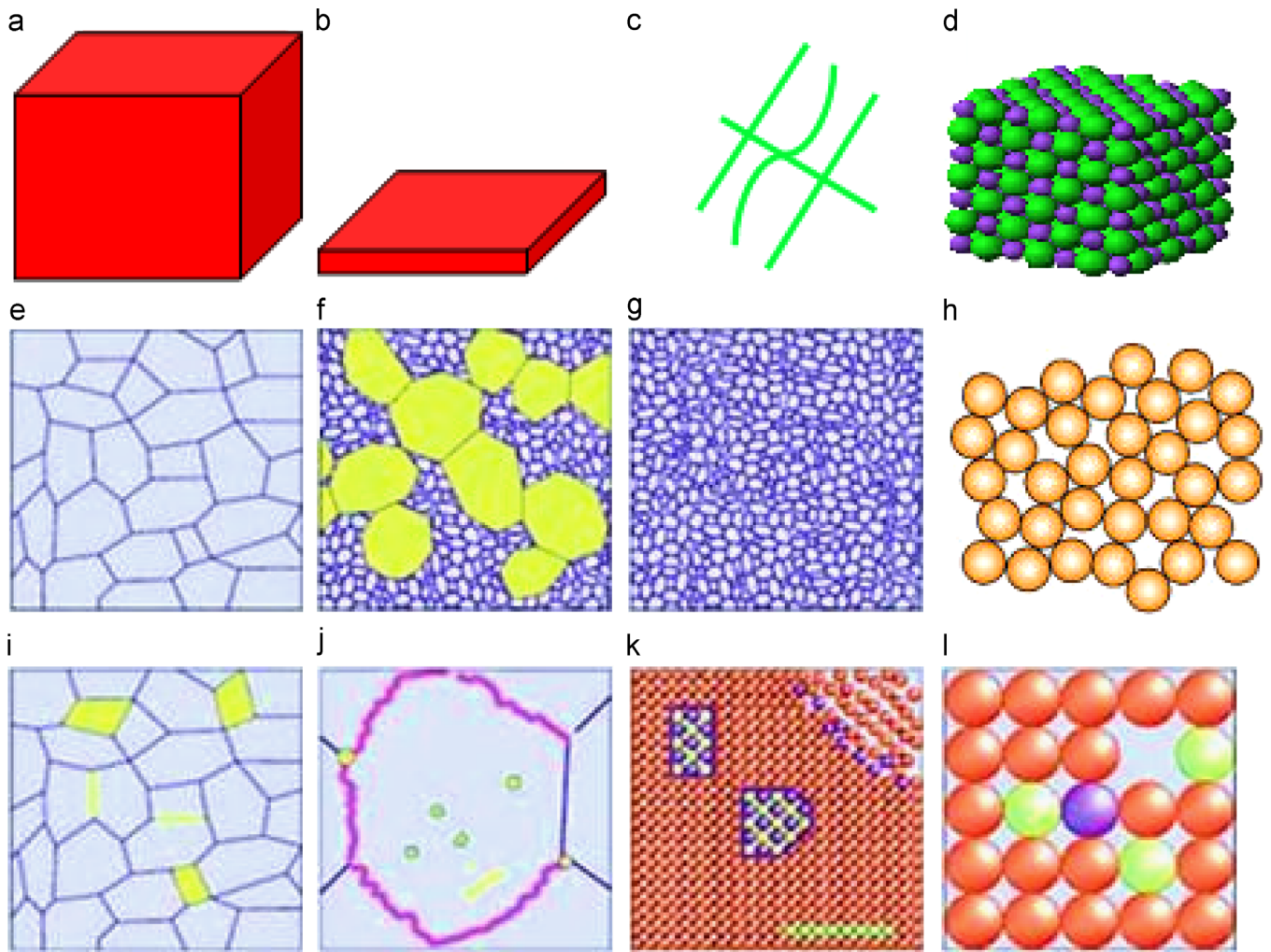
Fig. 12. Summary of thermoelectric material structure from macro- to nanoscale. (a–d) Change in dimensionality: (a) bulk, (b) thin film, (c) nanowire, and (d) atomic cluster. (e–h) Grain mixtures from micro- to nanoscale: (e) normal micro-grained bulk, (f) mixture of coarse and fine grains, (g) nano-grained bulk, and (h) amorphous. (i–l) Size evolution of isolated distinct phases or atoms in the composite: (i) normal composite, (j) nanodispersions located inside grains or at grain boundaries, (k) nano-inclusions or nanodots, boundary modification, and (l) atomic doping or alloying, and vacancies [138].

Table 3

Comparison of maximum ZT values for bulk and nanostructured thermoelectric materials [135].

Material	Bulk		Nanostructured	
	ZT_{max}	Temperature at which ZT_{max} is observed	ZT_{max}	Temperature at which ZT_{max} is observed
Si	0.2	1200	0.7	1200
$Si_{80}Ge_{20}$ (n-type)	1.0	1200	1.3	1173
$Si_{80}Ge_{20}$ (p-type)	0.7	1200	0.93	1073
$(Bi,Sb)_2Te_3$	0.9	293	1.4	373
$CoSb_3$	0.45	700	0.71	700

Introducing an acoustically mismatched second phase in a matrix is another way to reduce the lattice thermal conductivity through an additional scattering mechanism. Fig. 12(i–l) gives an indication of the size reduction of isolated distinct phases or atoms in the composite, including sphere-, plate- and wire-shaped dispersed phases which can enhance the thermoelectric properties [138].

Summarly, bulk nanostructuring has become a favored remarkable method for enhancing the thermoelectric properties over those of bulk materials. Moreover, approaches such as ball milling, nanocomposite fabrication and acoustical mismatch of secondary phases in a bulk material matrix are attractive strategies of improving the thermoelectric figure of merit.

7. Doping modulation of $Mg_2Si_{1-x}Sn_x$ thermoelectric materials

In the previous section, reduction of dimensionality that has been considered for many studies to improve the thermoelectric performance at a relatively low cost has been discussed. More recently, element doping that has been employed to improve the thermoelectric performance of magnesium silicide materials has tuned the electrical and thermal properties by element doping or substitution [146]. Moreover, the doping of semiconductors material is promising to improve the electrical properties of thermoelectric materials without altering thermal conductivity [147].

In this context, improvement of $Mg_2(Si-Sn)$ thermoelectric material performance due to the effects of doping has been extensively investigated. In 2012, Du et al. [84] investigated $Mg_2Si_{0.58}Sn_{0.42}$ compounds by Bi doping, the electrical conductivity was increased with an increase in the Bi doping amount. In studies published by Zhang et al. [62] on $Mg_2(Si-Sn)$ thermoelectric materials doped with La, the Mg2Si-rich bulk grains were
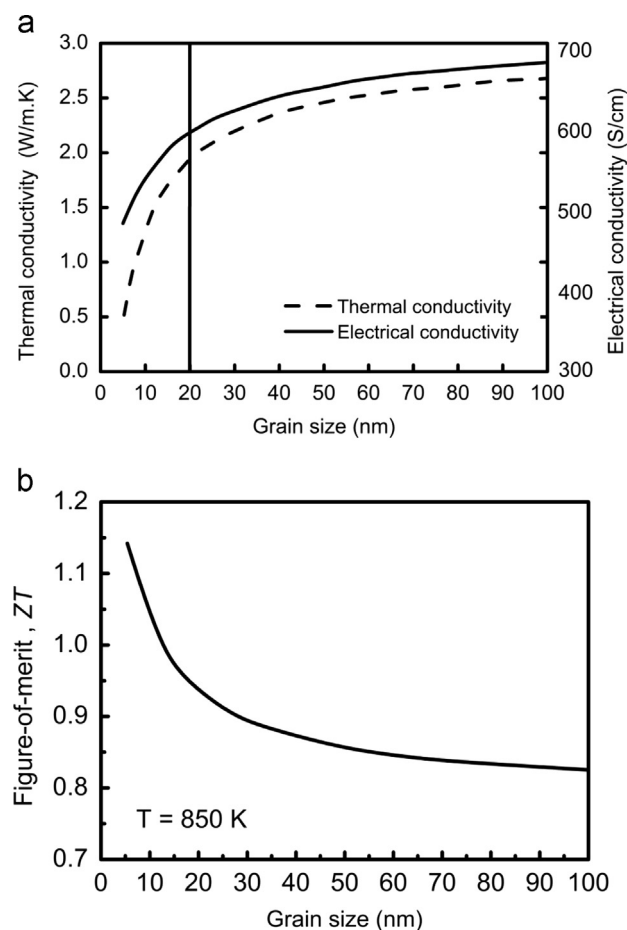
Fig. 13. (a) Comparison of calculated electrical conductivity and thermal conductivity of nanostructured Mg_2Si versus grain size and (b) variation of figure of merit with grain size in Mg_2Si [143].

in situ coated by Mg_2Sn-rich thin layers, and they demonstrated a ZT value of 0.81 at 810 K. Another study was carried out by Zaitsev et al. [148] on $Mg_2Si_{0.4}Sn_{0.6}$ Sb-doped compounds, the results showed that $Mg_2Si_{0.4}Sn_{0.6}$ is the most promising system for the development of thermoelectric efficiency through doping with the Sb element, and achieved a $ZT \approx 1.1$ at 800 K.

Moreover, recent studies published by Liu et al. [41] on $Mg_{2.16}Si_{0.4}Sn_{0.6}$ solid solution and adding Sb as a dopant indicated that the Sb doping is able to enhance the electrical conductivity of the material over the whole temperature range, they possessed excellent thermoelectric properties and achieved a high ZT value of 1.3 at 740 K. In 2013, in studies conducted by Liu et al. [149] on $Mg_{2.16}Si_{0.4}Sn_{0.6}$ solid solutions doped by Bi, the results showed an improvement of about 10% in comparison to values obtained by [41] with the Sb-dopant. This improvement comes chiefly from a marginally higher Seebeck coefficient of Bi-doped solid solutions. The highest $ZT = 1.4$ is achieved at 800 K. Furthermore, several experimental studies on Mg_2(Si–Sn) based composites show that the thermoelectric properties have been enhanced by appropriate types of dopants. Therefore, the element doping significantly influences the transport properties of the materials; through an increase in the carrier concentration, which impacts the electrical conductivity and subsequently the overall power factor of these thermoelectric materials. Doping techniques considerably decrease the lattice thermal conductivity, particularly in the high temperature range [86]. All the results show that doping technique for enhancement of thermoelectric performance for Mg_2(Si–Sn) based composites is reliable.

8. Applications of $Mg_2Si_{1-x}Sn_x$ thermoelectric materials' device

In 1996, the U.S. Air Force conducted a survey on thermal considerations on the performance of electronic systems. The results indicated that more than 50% of the electronic failures are related to temperature [150]. For example, significant waste heat is emitted from electronic domestic appliances, automobile electronics, computers and portable electronics. The thermoelectric system is a promising method to convert these waste heat energy into useful energy power without causing pollution or extra energy consumption during operation [151]. Utilization of waste heat as a potential source of electricity is a potentially "green" technology when the raw materials that are environmentally benign, the fabrication processes are energetically conservative and the end of life issues are managed in an environmentally compatible manner. Furthermore, tapping ambient waste heat cushions the effect of environmental warming as this waste heat is channeled into useful applications. As such, thermoelectric technology is being harnessed in applications such as thermoelectric cooling (TEC), thermoelectric heating (TEH) and thermoelectric power generation (TEG) [152–154].

For TEH and TEC configurations based on the Peltier effect, a voltage difference is applied through the object, leading to a control of the temperature difference [155]. The majority of the applications of thermoelectric devices have been used for cooling purposes. Normally, the heat of the object is absorbed by the cold side of the thermoelectric module, and the hot side of the module is attached to a heat sink in order to reject this heat into the atmosphere. TEC devices have been widely used in electronic equipment such as diode lasers, IR detectors, car seats and refrigerators [156–159], where the modules provide a fast and precise control of temperature, and are noise-free during operation [160]. In the other direction, semiconductor thermoelectric heat pumping (TEH) is a very interesting technology that has the capability to compete with conventional heat pumping systems [161,162]. The thermoelectric heat pump (TEH) is a heating device which potentially provides cost savings due to its relatively high efficiency when compared to resistance heating device. TEH devices have been developed for applications such as clothes' dryers, water heaters, and incubators [163]. Furthermore, they have the potential to be used in specific applications including the military, areospace, instrument, biology, medicine and industrial or commercial products [164,165]. The thermoelectric heat pump has the advantage over for traditional heat pump in terms of lower noise level and compressor vibration, and reduction in weight and size [162].

Thermoelectric generators (TEGs) modules for waste heat conversion consist of arrays of p-type and n-type semiconducting junctions which are electrically in series and thermally in parallel, as shown in Fig. 14 [166]. Given its scalability, TEGs may be utilized to suit a range of power needs. On the miliwatt scale, TEGs have the potential to supply power to low power applications such as wireless sensors, mobile devices, and even medical applications [167,168]. In 1998, Seiko incorporated thermoelectric into wristwatches, which utilizes thin bulk thermoelectric devices driven by body heat, the result the energy consumption reduced of approximately 1 μW [22]. TEGs have also been used in domestic situations such as waste heat recovery for woodstoves and diesel power plants [169]. Bi–Te TEG modules are already commercially available, such as those manufactured by Komatsu and Ferrotec [43]. Since the recognition of the potential of Mg_2Si as thermoelectric materials, silicides based TEG modules are currently being developed by Murata Corporation [170].

In order to develop commercial Mg_2(Si–Sn) TEG modules, balanced p-type and n-type materials must be readily available.
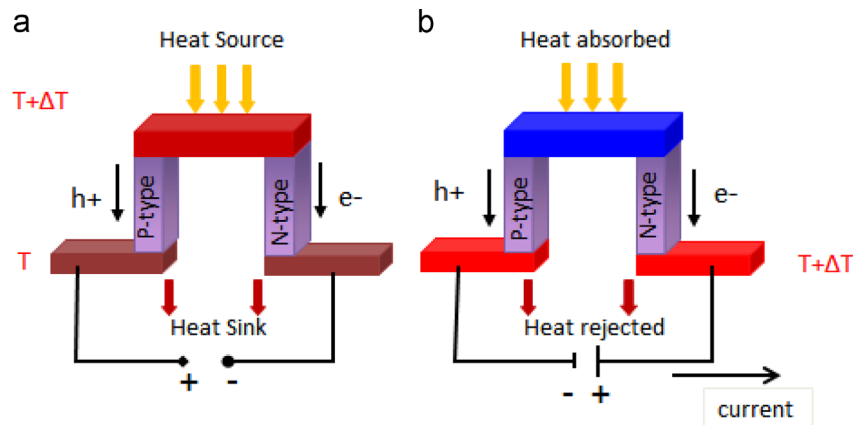
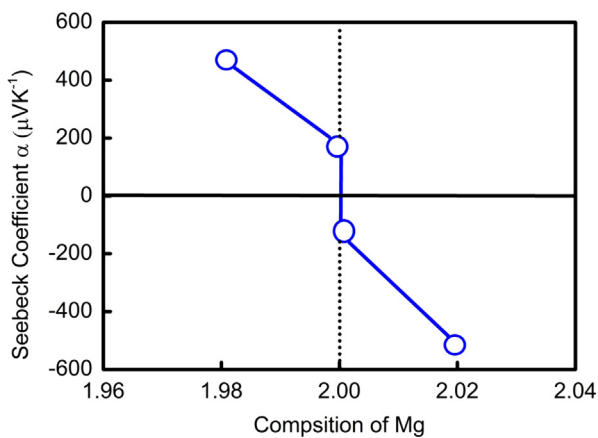**Fig. 14.** Basic thermoelectric device for (a) heat-to-electrical energy conversion and (b) heat pumping [166].

Fig. 15. Seebeck coefficient as a function of magnesium composition for $Mg_xSi_{0.25}Sn_{0.75}$ at room temperature [119].

Most of the Mg_2(Si–Sn) material solid solutions display favorable n-type thermoelectric properties in the temperature range of 500–900 K [171]. On the other hand, the preparation of a stoichiometric composition with p-type conduction is very difficult. Fig. 15 gives an idea of p-type and n-type $Mg_xSi_{0.25}Sn_{0.75}$ stoichiometric composition solid solutions with their corresponding Seebeck coefficient [119]. Studies were conducted by Nemoto et al. [172] on thermoelectric modules, which are composed only of n-type Sb-doped Mg_2Si legs, of dimensions of 21 mm × 30 mm × 16 mm. The results showed a ZT value of 0.77 at 862 K and the observed values of the open-circuit voltage and output power were 496 mV and 1211 mW, respectively at $\Delta T=531$ K. Kaibe et al. [173] have successfully implemented silicide thermoelectric modules consisting of p-$MnSi_{1.73}$ and n-$Mg_2Si_{0.4}Sn_{0.6}$, both doped with Sb. The results showed that the efficiency more than 6.5% at $T_h=550$ with $T_c=30$ has been obtained.

9. Efficiency of thermoelectric devices

Despite the initial promise of TEGs for waste heat harvesting into electricity, currently the applications are extremely limited by their inefficiency. The efficiency of a thermoelectric device depends on several factors other than the maximum figure of merit, ZT, of the materials. The system efficiency at maximum power output is inversely proportional to the sum of the heat dissipation of the resistances of the hot and cold terminals in the TEG modules [174]. The technical report from Komatsu mentioned

that the conversion efficiency, η, of their TEG modules are between 12% and 15% over a wide temperature range, from room temperature to around 600 °C [43]. The overall efficiency of a thermoelectric generator device η is limited by the Carnot cycle and the ZT figure of merit of the entire device and depends on the temperature difference $\Delta T=(T_h-T_c)$ across the device, which accounts for the individual ZT of the n- and p-type legs from [175]

$$\eta = (\Delta T/T_h). ((\sqrt{(1+ZT)}-1)/(\sqrt{(1+ZT)}+(T_c/T_h))) \qquad (16)$$

$\Delta T=(T_h-T_c)$ is the temperature difference at hot and cold sides. Like all heat engines, the maximum power-generation efficiency of a thermoelectric generator is thermodynamically limited by the Carnot efficiency ($\Delta T/T_h$). Therefore the efficiency of a thermoelectric device, operating in a cooling or refrigeration method, is expressed by the following coefficient of performance (COP) [176]:

$$COP = (\text{heat absorbed})/(\text{electrical power input}) \qquad (17)$$

The COP of thermoelectric cooling or refrigeration is lower than the conventional refrigeration techniques approximately by a factor of 0.5 [177]. Approximately 90% of the commercially available thermoelectric modules are manufactured from bismuth telluride because it exhibits TE efficiency in the range of 6–8% [38,39]. However, the disadvantages of Bi_2Te_3 compounds are inherent toxicity and limited chemical stability at high temperatures in air [166]. Magnesium silicides, having been considered as alternative thermoelectric materials, have demonstrated that TEGs with an element efficiency of 6.4% have reportedly been achieved using a combination of microstructure-controlled $MnSi_{1.73}$ (p-type) and Mg_2Si (n-type) [16]. Furthermore, the efficiency two-segmented thermoelectric modules fabricated from n-type $Mg_2(Si_{0.3}Sn_{0.7})_{1-x}Sb_x$ based materials reached the highest efficiency of about 8.5% at the range of temperature 323–773 K at a power of 19.9 W [178]. To achieve the initial promise of TEGs as commercially viable energy harvesting devices, a dimensionless figure of merit ZT of greater than unity and relevant to 10% conversion efficiency will be required [4]. The beneficial effect of using thermoelectric power generation can be taken by example of its application in diesel engines, where around 43 MW/h, or 167 GWh per annum of power savings can be achieved. This corresponds to crude oil savings of 40,600 kl/year, and the reduction of CO_2 emission is approximately by 20,200 t/year [43]. Given the promise of such improvements in the global energy consumption and reduction in greenhouse gases, the search for Mg_2(Si–Sn) remains a viable candidate for commercial thermoelectric materials.

10. Conclusion

This review summarizes the recent progress of Mg₂Si–Sn materials as a contender for thermoelectric applications, especially in the mid-temperature range of 500–900 K. The thermoelectric performance of this class of materials has been reviewed in terms of the material parameters, i.e. thermal and electrical conductivities, Seebeck coefficient and power factor. The development of these materials has been discussed, especially in terms of nanostructuring and element doping approaches. Among these methods, ball milling, hot pressing and spark plasma sintering have been identified as well-established techniques to achieve fine-grained structures, which serve to improve the thermoelectric figure of merit and subsequently allow for a large-scale production of these materials for commercial applications. The material advantages of these classes of materials, such as availability of raw resources, lowered material and production costs, relatively high figure of merit and lack of toxicity, have furthered their potential as a next generation materials in thermoelectric generator applications.

Acknowledgments

References

[1] Sootsman JR, Chung DY, Kanatzidis MG. New and old concepts in thermoelectric materials. Angew Chem 2009;48:8616–39.
[2] Bell LE. Cooling, heating, generating power, and recovering waste heat with thermoelectric systems. Science 2008;321:1457–61.
[3] Martín-González M, Caballero-Calero O, Díaz-Chao P. Nanoengineering thermoelectrics for 21st century: energy harvesting and other trends in the field. Renew Sustain Energy Rev 2013;24:288–305.
[4] Yoshinaga M, Iida T, Noda M, Endo T, Takanashi Y. Bulk crystal growth of Mg₂Si by the vertical Bridgman method. Thin Solid Films 2004;461:86–9.
[5] Ullah KR, Saidur R, Ping HW, Akikur RK, Shuvo NH. A review of solar thermal refrigeration and cooling methods. Renew Sustain Energy Rev 2013;24:499–513.
[6] Fthenakis V, Kim HC. Life-cycle uses of water in U.S. electricity generation. Renew Sustain Energy Rev 2010;14:2039–48.
[7] Chen F, Lu S-M, Tseng K-T, Lee S-C, Wang E. Assessment of renewable energy reserves in Taiwan. Renew Sustain Energy Rev 2010;14:2511–28.
[8] Chen Z, Han G, Yang L, Cheng L, Zou J. Nanostructured thermoelectric materials: current research and future challenge. Prog Nat Sci: Mater Int 2012;22:535–49.
[9] Hayakawa Y, Arivanandhan M, Saito Y, Koyama T, Momose Y, Ikeda H, et al. Growth of homogeneous polycrystalline Si₁₋ₓGeₓ and Mg₂Si₁₋ₓGeₓ for thermoelectric application. Thin Solid Films 2011;519:8532–7.
[10] Dmitriev AV, Zvyagin IP. Current trends in the physics of thermoelectric materials. Physics—Uspekhi 2010;53:789–803.
[11] Ali MB, Saidur R, Hossain MS. A review on emission analysis in cement industries. Renew Sustain Energy Rev 2011;15:2252–61.
[12] Kalkan N, Young EA, Celiktas A. Solar thermal air conditioning technology reducing the footprint of solar thermal air conditioning. Renew Sustain Energy Rev 2012;16:6352–83.
[13] Afshar O, Saidur R, Hasanuzzaman M, Jameel M. A review of thermodynamics and heat transfer in solar refrigeration system. Renew Sustain Energy Rev 2012;16:5639–48.
[14] Wang T, Zhang Y, Peng Z, Shu G. A review of researches on thermal exhaust heat recovery with Rankine cycle. Renew Sustain Energy Rev 2011;15:2862–71.
[15] Alam H, Ramakrishna S. A review on the enhancement of figure of merit from bulk to nano-thermoelectric materials. Nano Energy 2013;2:190–212.
[16] Kawamoto HR, Trends D. in high efficiency thermoelectric conversion materials for waste heat recovery. Sci Technol Trends 2009:54–69.
[17] Akasaka M, Iida T, Matsumoto A, Yamanaka K, Takanashi Y, Imai T, et al. The thermoelectric properties of bulk crystalline n- and p-type Mg₂Si prepared by the vertical Bridgman method. J Appl Phys 2008;104:013703.
[18] Tomeš P, Trottmann M, Suter C, Aguirre MH, Steinfeld A, Haueter P, et al. Thermoelectric oxide modules (TOMs) for the direct conversion of simulated solar radiation into electrical energy. Materials 2010;3:2801–14.
[19] Hmood A, Kadhim A, Hassan HA. Fabrication and characterization of Pb₁₋ₓYbₓTe-based alloy thin-film thermoelectric generators grown by thermal evaporation technique. Mater Sci Semicond Process 2013;16:612–8.
[20] Itoh T, Yamada M. Synthesis of thermoelectric manganese silicide by mechanical alloying and pulse discharge sintering. J Electron Mater 2009;38:925–9.
[21] Keskar G, Iyyamperumal E, Hitchcock DA, He J, Rao AM, Pfefferle LD. Significant improvement of thermoelectric performance in nanostructured bismuth networks. Nano Energy 2012;1:706–13.
[22] Kishi M, Nemoto H, Hamao T, Yamimoto M, Sudou S, Mandai M, et al. Micro thermoelectric modules and their application to wristwatches as anenergy source. In: Eighteenth international conference on thermoelectrics (ICT); 1999. p. 301–7.
[23] Ali MB, Saidur R, Hasanuzzaman M, Ward TA. Energy and emission analysis in the Malaysian food industries. Environ Prog Sustain Energy 2012;32:777–783.
[24] Balandin AA. Thermal properties of graphene and anostructured carbon materials. Nat Mater 2011;10:13.
[25] Toberer ES, May AF, Snyder GJ. Zintl chemistry for designing high efficiency thermoelectric materials. Chem Mater 2010;22:624–34.
[26] Cederkrantz D, Farahi N, Borup KA, Iversen BB, Nygren M, Palmqvist AEC. Enhanced thermoelectric properties of Mg₂Si by addition of TiO₂ nanoparticles. J Appl Phys 2012;111:023701.
[27] Omer AM. Focus on low carbon technologies: the positive solution. Renew Sustain Energy Rev 2008;12:2331–57.
[28] Kajikawa T. Overview of thermoelectric power generation technologies in Japan. Kanagawa, Japan: Shonan Institute of Technology; 2011.
[29] Bottner H. Thermoelectric activities of european community within framework programe 7 and additional activities in Germany. Third thermoelectric applications workshop; 2012. USA: Fraunhofer IPM.
[30] Liebl IEJ, Neugebauer IS. The thermoelectric generator from BMW is making use of waste heat. MTZ Worldwide 2009;70:4–11.
[31] Vining CB. An inconvenient truth about thermoelectrics. Nat Mater 2009:8.
[32] Jund P, Viennois R, Colinet C, Hug G, Fèvre M, Tédenac J. Lattice stability and formation energies of intrinsic defects in Mg₂Si and Mg₂Ge via first principles simulations. J Phys: Condens Matter 2013;25:035403.
[33] Szczech JR, Higgins JM, Jin S. Enhancement of the thermoelectric properties in nanoscale and nanostructured materials. J Mater Chem 2011;21:4037.
[34] Savary E, Gascoin F, Marinel S, Heuguet R. Spark plasma sintering of fine Mg₂Si particles. Powder Technol 2012;228:295–300.
[35] Elsheikh MH, Shnawah DA, Sabri MFM, Said SBM, Haji Hassan M, Bashir MBA, et al. A review on thermoelectric renewable energy: principle parameters that affect their performance. Renew Sustain Energy Rev 2014;30:337–55.
[36] An T-H, Choi S-M, Kim I-H, Kim S-U, Seo W-S, Kim J-Y, et al. Thermoelectric properties of a doped Mg₂Sn system. Renew Energy 2012;42:23–7.
[37] Gao X, Uehara K, Klug D, Tse J. Rational design of high-efficiency thermoelectric materials with low band gap conductive polymers. Comput Mater Sci 2006;36:49–53.
[38] Stranz A, Sokmen U, Kähler J, Waag A, Peiner E. Measurements of thermoelectric properties of silicon pillars. Sens Actuators 2011;171:48–53.
[39] Yang J. Potential applications of thermoelectric waste heat recovery in the automotive industry. In: International conference on thermoelectrics. IEEE; Clemson, SC, USA, 2005. p. 155–9.
[40] Liu W, Zhang Q, Tang X, Li H, Sharp J. Thermoelectric properties of Sb-doped Mg₂Si₀.₃Sn₀.₇. J Electron Mater 2011;40:1062–6.
[41] Liu W, Tang X, Li H, Yin K, Sharp J, Zhou X, et al. Enhanced thermoelectric properties of n-type Mg₂.₁₆ (Si₀.₄Sn₀.₆)₁₋ᵧSbᵧ due to nano-sized Sn-rich precipitates and an optimized electron concentration. J Mater Chem 2012;22:13653.
[42] LeBlanc S, Yee SK, Scullin ML, Dames C, Goodson KE. Material and manufacturing cost considerations for thermoelectrics. Renew Sustain Energy Rev 2014;32:313–27.
[43] Sano S, Mizukami H, Kaibe H. Development of high-efficiency thermoelectric power generation system. Komatsu 2003:1–7.
[44] Rowe DM. Review thermoelectric waste heat recovery as a renewable energy source. Int J Innov Energy Syst Power 2006;1:13–23.
[45] Gao H, Zhu T, Liu X, Chen L, Zhao X. Flux synthesis and thermoelectric properties of eco-friendly Sb doped Mg₂Si₀.₅Sn₀.₅ solid solutions for energy harvesting. J Mater Chem 2011;21:5933.
[46] Chen R. Silicide nanopowders as low-cost and high-performance thermoelectric materials. JOM 2013;65:702–8.
[47] Zhang SN, Zhu TJ, Yang SH, Yu C, Zhao XB. Improved thermoelectric properties of AgSbTe₂ based compounds with nanoscale Ag₂Te in situ precipitates. J Alloys Compd 2010;499:215–20.
[48] Gao HL, Liu XX, Zhu TJ, Yang SH, Zhao XB. Effect of Sb doping on the thermoelectric properties of Mg₂Si₀.₇Sn₀.₃ solid solutions. J Electron Mater 2011;40:830–4.
[49] Zhang Q, Zhao XB, Yin H, Zhu TJ. Thermoelectric performance of Mg₂₋ₓCaₓSi compounds. J Alloys Compd 2008;464:9–12.
[50] Hummel RE. Electronic properties of materials. 3rd ed. New York: Springer; 2000.
[51] Joshi G. Study of thermoelectric properties of nanostructured p-type Si–Ge, Bi–Te, Bi–Sb, and halfheusler bulk materials. ProQuest LLC: Boston College; 2010.
[52] Kang Y, Brockway L, Vaddiraju S. A simple phase transformation strategy for converting silicon nanowires into metal silicide nanowires: magnesium silicide. Mater Lett 2013;100:106–10.

[53] Zheng XJ, Zhu L, Zhou Y, Zhang Q. Impact of grain sizes on phonon thermal conductivity of bulk thermoelectric materials. Appl Phys Lett 2005;87:242101.

[54] Pulikkotil JJ, Alshareef HN, Schwingenschlogl U. Variation of equation of state parameters in the $Mg_2(Si_{(1-x)}Sn_{(x)})$ alloys. J Phys: Condens Matter 2010;22:3.

[55] Majumdar A. Thermoelectricity in semiconductor nanostructures. Science 2004;303:777–8.

[56] Tritt TM. Thermal conductivity theory, properties, and applications. New York, USA: Springer; 2004.

[57] Koza MM, Johnson MR, Viennois R, Mutka H, Girard L, Ravot D. Breakdown of phonon glass paradigm in La- and Ce-filled Fe_4Sb_{12} skutterudites. Nat Mater 2008;7:805–10.

[58] Thiagarajan SJ, Wang W, Yang R. Nanocomposites as high efficiency thermoelectric materials. In: Guozhong C, Zhang Q, Brinker CJ, editors. Annual review of nano research. World Scientific, Boulder, CO, USA; 2010. p. 555.

[59] Bux SK, Fleurial JP, Kaner RB. Nanostructured materials for thermoelectric applications. Chem Commun 2010;46:8311–24.

[60] Medlin DL, Snyder GJ. Interfaces in bulk thermoelectric materials. Curr Opin Colloid Interface Sci 2009;14:226–35.

[61] Liu W, Tan X, Yin K, Liu H, Tang X, Shi J, et al. Convergence of conduction bands as a means of enhancing thermoelectric performance of n-type $Mg_2Si_{1-x}Sn_x$ solid solutions. Phys Rev Lett 2012:108.

[62] Zhang Q, He J, Zhao XB, Zhang SN, Zhu TJ, Yin H, et al. in situsynthesis and thermoelectric properties of La-doped $Mg_2(Si, Sn)$ composites. J Phys D: Appl Phys 2008;41:185103.

[63] Ioannou M, Polymeris G, Hatzikraniotis E, Khan AU, Paraskevopoulos KM, Kyratsi T. Solid-state synthesis and thermoelectric properties of Sb-doped Mg_2Si materials. J Electron Mater 2013;42:1827–34.

[64] Song RB, Aizawa T, Sun JQ. Synthesis of $Mg_2Si_{1-x}Sn_x$ solid solutions as thermoelectric materials by bulk mechanical alloying and hot pressing. Mater Sci Eng: B 2007;136:111–7.

[65] Du ZL, Jiang GY, Chen Y, Gao HL, Zhu TJ, Zhao XB. Effect of GaSb addition on the thermoelectric properties of $Mg_2Si_{0.5}Sn_{0.5}$ solid solutions. J Electron Mater 2012;41:1222–6.

[66] Goldsmid HJ. Introduction to thermoelectricity. New York: Springer; 2009.

[67] Chen X, Weathers A, Moore A, Zhou J, Shi L. Thermoelectric properties of cold-pressed higher manganese silicides for waste heat recovery. J Electron Mater 2012;41:1564–72.

[68] Kumar G, Prasad G, Ro Pohl. Review experimental determinations of the Lorenz Number. J Mater Sci 1993:4261–72.

[69] Tan XJ, Liu W, Liu HJ, Shi J, Tang XF, Uher C. Multiscale calculations of thermoelectric properties of n-type $Mg_2S_{1-x}Sn_x$ solid solutions. Phys Rev B 2012:85.

[70] Noda Y, Kon H, Furukawa Y, Nishida IA, Masumoto K. Temperature dependence of thermoelectric properties of $Mg_2Si_{0.6}Ge_{0.4}$. Mater Trans, JIM 1992;33:851–5.

[71] Sharp JW. Selection and evaluation of materials for thermoelectric applications II. Mater Res Soc 1997:478.

[72] Jeng M-S, Yang R, Song D, Chen G. Modeling the thermal conductivity and phonon transport in nanoparticle composites using monte carlo simulation. J Heat Transfer 2008;130:11.

[73] Zaitsev V, Fedorov M, Gurieva E, Eremin I, Konstantinov P, Samunin AY, et al. Highly effective $Mg_2Si_{1-x}Sn_x$ thermoelectrics. Phys Rev B 2006;74:045207.

[74] Zhang Q, He J, Zhu TJ, Zhang SN, Zhao XB, Tritt TM. High figures of merit and natural nanostructures in $Mg_2Si_{0.4}Sn_{0.6}$ based thermoelectric materials. Appl Phys Lett 2008;93:102–9.

[75] Zhu T-J, Cao Y-Q, Zhang Q, Zhao X-B. Bulk nanostructured thermoelectric materials: preparation, structure and properties. J Electron Mater 2009;39:1990–5.

[76] Tritt TM. Thermoelectric materials—new directions and approaches. In: Tritt TM, Kanatzidis MG, Hylan B, Lyon J, Mahan GD, editors. Pennsylvania, USA: Materials Research Society; 1997.

[77] Li SS. Semiconductor physical electronics. 2nd ed. New York: Springer; 2006.

[78] Du Z, Zhu T, Chen Y, He J, Gao H, Jiang G, et al. Roles of interstitial Mg in improving thermoelectric properties of Sb-doped $Mg_2Si_{0.4}Sn_{0.6}$ solid solutions. J Mater Chem 2012;22:6838.

[79] Isoda Y, Nagai T, Fujiu H, Imai Y, Shinohara Y. The effect of Bi doping on thermoelectric properties of $Mg_2Si_{0.5}Sn_{0.5}$. In: International conference on thermoelectrics; 2008. p. 251–5.

[80] You S-W, Kim I-H, Choi S-M, Seo W-S. Solid-state synthesis and thermoelectric properties of $Mg_{2+x}Si_{0.7}Sn_{0.3}Sb_m$. J Nanomater 2013;2013:1–4.

[81] Nolas G, Morelli D, Tritt T. Skutterudites: a phonon–glass–electron crystal approach to advanced thermoelectric energy conversion applications. Annu Rev Mater Sci 1999;29:89–116.

[82] Tritt T, Subramanian M. Thermoelectric materials, phenomena, and applications. A bird's eye view. MRS Bull 2006;31:188–229.

[83] Shaheen A, Zia W, Khalid A, Anwar MS. Band structure and electrical conductivity in semiconductors. Lahore, Pakistan: LUMS School of Science and Engineering; 2011.

[84] Du Z, Zhu T, Zhao X. Enhanced thermoelectric properties of $Mg_2Si_{0.58}Sn_{0.42}$ compounds by Bi doping. Mater Lett 2012;66:76–8.

[85] Tani J-i Kido H. Thermoelectric properties of Sb-doped Mg_2Si semiconductors. Intermetallics 2007;15:1202–7.

[86] Liu W, Tang X, Sharp J. Low-temperature solid state reaction synthesis and thermoelectric properties of high-performance and low-cost Sb-doped $Mg_2Si_{0.6}Sn_{0.4}$. J Phys D: Appl Phys 2010;43:085406.

[87] Liu W, Tang X, Li H, Sharp J, Zhou X, Uher C. Optimized thermoelectric properties of Sb-doped $Mg_{2(1+z)}Si_{0.5-y}Sn_{0.5}Sb_y$ through adjustment of the Mg content. Chem Mater 2011;23:5256–63.

[88] Snyder GJ, Toberer ES. Complex thermoelectric materials. Nat Mater 2008;7:105–14.

[89] Valset K. Studies of electronic structure and thermal properties of thermoelectric materials emphasising quantitative electron diffraction [PhD thesis]. University of Oslo; 2011.

[90] Wang S, Fu F, She X, Zheng G, Li H, Tang X. Optimizing thermoelectric performance of Cd-doped β-Zn_4Sb_3 through self-adjusting carrier concentration. Intermetallics 2011;19:1823–30.

[91] Ozpineci B, Tolbert LM. Comparison of wide-bandgap semiconductors for power electronics applications. United States: Department of Energy; 2003.

[92] Nielsch K, Bachmann J, Kimling J, Bottner H. Thermoelectric nanostructures: from physical model systems towards nanograined composites. Adv Energy Mater 2011;1:713–31.

[93] Chen L, Jiang G, Chen Y, Du Z, Zhao X, Zhu T, et al. Miscibility gap and thermoelectric properties of ecofriendly $Mg_2Si_{1-x}Sn_x$ $(0.1 \leq x \leq 0.8)$ solid solutions by flux method. J Mater Res 2011;26:3038–43.

[94] Tripathi MN, Bhandari CM. Material parameters for thermoelectric performance. Pramana 2005;65:469–79.

[95] Le-Quoc H, Lacoste A, Béchu S, Bès A, Bourgault D, Fruchart D. Deposition of thin films of $Mg_2Si_{1-x}Sn_x$ solid solution by plasma-assisted co-sputtering. J Alloys Compd 2012;538:73–8.

[96] Viennois R, Jund P, Colinet C, Tédenac J. Defect and phase stability of solid solutions of Mg_2X with an antifluorite structure: an ab initio study. J Solid State Chem 2012;193:133–6.

[97] Pulikkotil JJ, Alshareef HN, Schwingenschlogl U. Variation of equation of state parameters in the $Mg_2(Si_{1-x}Sn_x)$ alloys. J Phys Condens Matter 2010;22:3.

[98] Lee HJ, Choa YR, Kim I. Synthesis of thermoelectric Mg_2Si by a solid state reaction. Ceram Process Res 2011;12:16–20.

[99] Liu W, Yin K, Su X, Li H, Yan Y, Tang X, et al. Enhanced hole concentration through Ga doping and excess of Mg and thermoelectric properties of p-type $Mg_{2(1+z)}(Si_{0.3}Sn_{0.7})_{1-y}Ga_y$. Intermetallics 2013;32:352–61.

[100] Godzhayev EM, Dzhafarova GS, Safarova SI Band structure of $TlInTe_2$ and thermoelectric figure of merit of solid solutions on its basis. J Thermoelectr 2013.

[101] Fedorov MI. Thermoelectric silicides past, present and future. J Thermoelectr 2009:51–60.

[102] Fedorov MI, Pshenay-Severin DA, Zaitsev VK, Sano S, Vedernikov MV. Features of conduction mechanism in n-type $Mg_2(Si_{1-x})Sn_x$ solid solutions. In: Twenty-second international conferance on thermoclcctrics (ICT). IEEE; France, 2003. p. 142–5.

[103] Zaitsev VK, Fedorov MI, Gurieva EA, Eremin IS., Konstantinov PP, Samunin AY, et al. Thermoelectrics of n-type with $ZT > 1$ based on Mg_2Si–Mg_2Sn solid solutions. In: International conference on thermoelectrics. IEEE; 2005. p. 189–95.

[104] Isachenko GN, Zaitsev VK, Fedorov MI, Gurieva EA, Eremin IS, Konstantinov PP, et al. The study of p-type material based on Sn-rich Mg_2Si–Mg_2Sn solid solution. In: Twenty-sixth international conference on thermoelectrics (ICT 2007). IEEE; Jeju Island, Korea (South), 2007. p. 248–50.

[105] Zhang X, Lu Q-m, Wang L, Zhang F-p, Zhang J-x. Preparation of $Mg_2Si_{1-x}Sn_x$ by induction melting and spark plasma sintering, and thermoelectric properties. J Electron Mater 2010;39:1413–7.

[106] Zhang Q, Zhu TJ, Zhou AJ, Yin H, Zhao XB. Preparation and thermoelectric properties of $Mg_2Si_{1-x}Sn_x$. Phys Scr 2007;T129:123–6.

[107] Fedorov MI, Zaitsev VK, Isachenko GN. High effective thermoelectrics based on the Mg_2Si–Mg_2Sn solid solution. In: Seventeenth international conference on solid compounds of transition elements. Durnten-Zurich: Trans Tech; 2011. p. 286–92.

[108] Fedorov MI, Zaĭtsev VK, Eremin IS, Gurieva EA, Burkov AT, Konstantinov PP, et al. Transport properties of $Mg_{2 \times 0.4}Sn_{0.6}$ solid solutions (X=Si, Ge) with p-type conductivity. Phys Solid State 2006;48:1486–90.

[109] Aizawa T, Song R, Yamamoto A. Solid state synthesis of ternary thermoelectric magnesium alloy, $Mg_2Si_{1-x}Sn_x$. Mater Trans 2006;47:1058–65.

[110] Chen HY, Savvides N. Microstructure and thermoelectric properties of n- and p-type doped Mg_2Sn compounds prepared by the modified bridgman method. J Electron Mater 2009;38:1056–60.

[111] Chen HY, Savvides N. Eutectic microstructure and thermoelectric properties of Mg_2Sn. J Electron Mater 2010;39:1792–7.

[112] Léonard F, Talin AA. Electrical contacts to one and two dimensional nanomaterials. Nat Nanotechnol 2011;9:773–83.

[113] Tani J, Kido H. Fabrication and thermoelectric properties of Mg_2Si-based composites using reduction reaction with additives. Intermetallics 2013;32:72–80.

[114] Yang MJ, Zang LM, Han LQ, Shen Q, Wang CB. Simple fabricatoin of Mg_2Si thermoelectric generator by spark plasma sintering. Indian J Eng Mater Sci 2009;16:277–80.

[115] Singh MP, Bhandari CM. High-temperature thermoelectric behavior of lead telluride. J Phys 2004;62:1309–17.

[116] Riffel M, Schilz J. Mechanically alloyed $Mg_2Si_{1-x}Sn_x$ solid solutions as thermoelectric materials. In: Fifteenth international conference on thermoelectrics. IEEE; Pasadena, CA, USA, 1996.

[117] Meng QS, Fan WH, Chen RX, Munir ZA. Thermoelectric properties of Sc- and Y-doped Mg_2Si prepared by field-activated and pressure-assisted reactive sintering. J Alloys Compd 2011;509:7922–6.

[118] Samunin AY, Zaitsev VK, Konstantinov PP, Fedorov MI, Isachenko GN, Burkov AT, et al. Thermoelectric properties of hot-pressed materials based on $Mg_2Si_nSn_{1-n}$. J Electron Mater 2012;42:1676–9.

[119] Isoda Y, Tada S, Nagai T, Fujiu H, Shinohara Y. Thermoelectric properties of p-type $Mg_{2.0}Si_{0.25}Sn_{0.75}$ with Li and Ag double doping. J Electron Mater 2010;39:1531–5.

[120] Grasso S, Reece M. High-Tech Sintering London: Ceramic Industry Magazine; 2012.

[121] Kopeliovich D. Spark plasma sintering. Substances & technologies 2013. Available online at: ⟨http://www.substech.com/dokuwiki/doku.php?id=spark_plasma_sintering⟩ [accessed 25.07.13].

[122] Han Z, Zhang X, Lu Q, Zhang J, Zhang F. Preparation and thermoelectric properties of $(Mg_2Si_{1-x}Sb_x)_{0.4}$–$(Mg_2Sn)_{0.6}$ alloys. J Inorg Mater 2012;27:822–6.

[123] Tani J-i Kido H. Thermoelectric properties of Al-doped $Mg_2Si_{1-x}Sn_x$ ($x \le 0.1$). J Alloys Compd 2008;466:335–40.

[124] Ganguly S, Zhou C, Morelli D, Sakamoto J, Uher C, Brock SL. Synthesis and evaluation of lead telluride/bismuth antimony telluride nanocomposites for thermoelectric applications. J Solid State Chem 2011;184:3195–201.

[125] Barron KC. Experimental studies in the thermoelectric properties of micro-structured and nanostructured lead salts [Bachelor thesis]. Massachusetts Institute of Technology; 2005.

[126] Ioannou M, Hatzikraniotis E, Lioutas C, Hassapis T, Altantzis T, Paraskevopoulos KM, et al. Fabrication of nanocrystalline Mg_2Si via ball milling process: structural studies. Powder Technol 2012;217:523–32.

[127] Ni HL, Zhao XB, Zhu TJ, Ji XH, Tu JP. Synthesis and thermoelectric properties of Bi_2Te_3 based nanocomposites. J Alloys Compd 2005;397:317–21.

[128] Chen G. Nanoscale heat transfer and nanostructured thermoelectrics. IEEE Trans Compon Packag Technol 2006;29:238–46.

[129] Kumpeerapun T, Hirunlabh J, Khedari J, Scherrer H, Kosalathip V, Phangream W, et al. Preparation of nanostructures thermoelectric materials using PLA technique. IEEE; Hong Kong, 2010.

[130] Humphrey T, Linke H. Reversible thermoelectric nanomaterials. Phys Rev Lett 2005:94.

[131] Wang X, Yang Y, Zhu L. Effect of grain sizes and shapes on phonon thermal conductivity of bulk thermoelectric materials. J Appl Phys 2011;110:024312.

[132] Hicks L, Dresselhaus M. Effect of quantum-well structures on the thermoelectric figure of merit. Phys Rev B 1993;47:12727.

[133] Dresselhaus MS, Chen G, Tang MY, Yang RG, Lee H, Wang DZ, et al. New directions for low-dimensional thermoelectric materials. Adv Mater 2007;19:1043–53.

[134] Je K-C, Cho C-H. Quantum confinement efect of thermoelectric properties. J Korean Phys Soc 2009;54:105–8.

[135] Vaqueiro P, Powell AV. Recent developments in nanostructured materials for high-performance thermoelectrics. J Mater Chem 2010;20:9577.

[136] Narducci D, Selezneva E, Cerofolini G, Frabboni S, Ottaviani G. Impact of energy filtering and carrier localization on the thermoelectric properties of granular semiconductors. J Solid State Chem 2012;193:19–25.

[137] Biswas K, He J, Blum ID, Wu CI, Hogan TP, Seidman DN, et al. High-performance bulk thermoelectrics with all-scale hierarchical architectures. Nature 2012;489:414–8.

[138] Li J-F, Liu W-S, Zhao L-D, Zhou M. High-performance nanostructured thermoelectric materials. NPG Asia Mater 2010;2:152–8.

[139] Nakagawa H, Tanaka H, Kasama A, Anno H, Matsubara K. Grain size effects on thermoelectric properties of hot-pressed $CoSb_3$. In: Sixteenth international conference on thermoelectrics. Dresden, Germany: IEEE; 1997.

[140] Suryanarayana C. Mechanical alloying and milling. Prog Mater Sci 2001;46:1–184.

[141] Pshenai-Severin DA, Fedorov MI, Samunin AY. The influence of grain boundary scattering on thermoelectric properties of Mg_2Si and $Mg_2Si_{0.8}Sn_{0.2}$. J Electron Mater 2013;42:1707–10.

[142] Wang XW, Lee H, Lan YC, Zhu GH, Joshi G, Wang DZ, et al. Enhanced thermoelectric figure of merit in nanostructured n-type silicon germanium bulk alloy. Appl Phys Lett 2008;93:193121.

[143] Satyala N, Vashaee D. Detrimental influence of nanostructuring on the thermoelectric properties of magnesium silicide. J Appl Phys 2012;112:093716.

[144] Mingo N, Hauser D, Kobayashi NP, Plissonnier M, Shakouri A. Nanoparticle-in-alloy approach to efficient thermoelectrics: silicides in SiGe. Nano Lett 2009;9:711–5.

[145] Peng H, Wang CL, Li JC, Wang HC, Sun Y, Zheng Q. Elastic and vibrational properties of $Mg_2Si_{1-x}Sn_x$ alloy from first principles calculations. Solid State Commun 2012;152:821–4.

[146] Zhou AJ, Zhao XB, Zhu TJ, Yang SH, Dasgupta T, Stiewe C, et al. Microstructure and thermoelectric properties of SiGe-added higher manganese silicides. Mater Chem Phys 2010;124:1001–5.

[147] Hou QR, Zhao W, Chen YB, Liang D, Feng X, Zhang HY, et al. Thermoelectric properties of higher manganese silicide films with addition of chromium. Appl Phys A 2006;86:385–9.

[148] Zaitsev V, Fedorov M, Gurieva E, Eremin I, Konstantinov P, Samunin AY, et al. Highly effective $Mg_2Si_{1-x}Sn_x$ thermoelectrics. Phys Rev B 2006;74:045207.

[149] Liu W, Zhang Q, Yin K, Chi H, Zhou X, Tang X, et al. High figure of merit and thermoelectric properties of Bi-doped $Mg_2Si_{0.4}Sn_{0.6}$ solid solutions. J Solid State Chem 2013;203:333–9.

[150] Yeh LT. Review of heat transfer technologies in electronic equipment. J Electron Packag 1996;117:7.

[151] Seo DK, Shin S, Cho HH, Kong BH, Whang DM, Cho HK. Drastic improvement of oxide thermoelectric performance using thermal and plasma treatments of the InGaZnO thin films grown by sputtering. Acta Mater 2011;59:6743–50.

[152] Xi H, Luo L, Fraisse G. Development and applications of solar-based thermoelectric technologies. Renew Sustain Energy Rev 2007;11:923–36.

[153] Leephakpreeda T. Applications of thermoelectric modules on heat flow detection. ISA Trans 2012;51:345–50.

[154] Caplain I, Cazier F, Nouali H, Mercier A, Déchaux J-C, Nollet V, et al. Emissions of unregulated pollutants from European gasoline and diesel passenger cars. Atmos Environ 2006;40:5954–66.

[155] Goupil C, Seifert W, Zabrocki K, Müller E, Snyder GJ. Thermodynamics of thermoelectric phenomena and applications. Entropy 2011;13:1481–517.

[156] Abdul-Wahab SA, Elkamel A, Al-Damkhi AM, IhA Al-Habsi, Al-Rubai'ey HS, Al-Battashi AK, et al. Design and experimental investigation of portable solar thermoelectric refrigerator. Renew Energy 2009;34:30–4.

[157] Zhao LD, Zhang BP, Liu WS, Zhang HL, Li JF. Effects of annealing on electrical properties of n-type Bi_2Te_3 fabricated by mechanical alloying and spark plasma sintering. J Alloys Compd 2009;467:91–7.

[158] Hirota M, Ohta Y, Fukuyama Y. Low-cost thermo-electric infrared FPAs and their automotive applications. Infrared Technol Appl 2008;XXXIV:6940.

[159] Yang J, Stabler FR. Automotive applications of thermoelectric materials. J Electron Mater 2009;38:1245–51.

[160] Li J-F, Tanaka S, Umeki T, Sugimoto S, Esashi M, Watanabe R. Microfabrication of thermoelectric materials by silicon molding process. Sens Actuators A: Phys 2003;108:97–102.

[161] Chen L, Li J, Sun F. Heat transfer effect on optimal performance of two-stage thermoelectric heat pumps. Proc Inst Mech Eng Part C: J Mech Eng Sci 2007;221:1635–41.

[162] Liu D, Zhao F-Y, Tang G-F. Active low-grade energy recovery potential for building energy conservation. Renew Sustain Energy Rev 2010;14:2736–47.

[163] Luo Q. Experimental study on thermoelectric heat pump for energy recovering and local heating in buildings. Int J Archit Sci 2005;6:173–7.

[164] Riffat SB, Ma X. Thermoelectrics: a review of present and potential applications. Appl Thermal Eng 2003;23:913–35.

[165] Barth S, Hernandez-Ramirez F, Holmes JD, Romano-Rodriguez A. Synthesis and applications of one-dimensional semiconductors. Prog Mater Sci 2010;55:563–627.

[166] Gorsse S, Bellanger P, Brechet Y, Sellier E, Umarji A, Ail U, et al. Nanostructuration via solid state transformation as a strategy for improving the thermoelectric efficiency of PbTe alloys. Acta Mater 2011;59:7425–37.

[167] Schmitt MC, Reith H, Huzel D, Volklein F. New measuring techniques for the investigation of thermoelectric properties of nanowires. In: nineth European Conference On Thermoelectrics: ECT; 2011, 385-388.

[168] Snyder GJ. Small thermoelectric generators. Electrochem Soc Interface 2008;17:54–6.

[169] Fergus JW. Oxide materials for high temperature thermoelectric energy conversion. J Eur Ceram Soc 2012;32:525–40.

[170] Kajitani T, Ueno T, Miyazaki Y, Hayashi K, Fujiwara T, Ihara R, et al. Fabrication of multilayer-type Mn–Si and Mg–Si thermoelectric devices. In: Thirty-second international conference on thermoelectrics ict proceedings; 2013.

[171] Isoda Y, Tada S, Nagai T, Fujiu H, Shinohara Y. Thermoelectric performance of p-type $Mg_2Si_{0.25}Sn_{0.75}$ with Li and Ag double doping. Mater Trans 2010;51:868–71.

[172] Nemoto T, Iida T, Sato J, Sakamoto T, Hirayama N, Nakajima T, et al. Development of an Mg_2Si unileg thermoelectric module using durable Sb-doped Mg_2Si legs. J Electron Mater 2013;42:2192–7.

[173] Kaibe HT, Rauscher L, Fujimoto S, Kurosawa T, Kanda T, Mukoujima M, et al. Development of thermoelectric generating cascade modules using silicide and Bi–Te. In: Twenty-third international conference on thermoelectrics, Australia; 2004. p. 13.

[174] Yazawa K, Shakouri A. Optimization of power and efficiency of thermoelectric devices with asymmetric thermal contacts. J Appl Phys 2012;111:024509.

[175] Müller E, Drašar Č, Schilz J, Kaysser WA. Functionally graded materials for sensor and energy applications. Mater Sci Eng: A 2003;362:17–39.

[176] Rowe DM. Thermoelectrics handbook: macro to nano. Boca Raton, FL: CRC Press; 2005; 1014.

[177] Gould C, Shammas N. A review of thermoelectric MEMS devices for micro-power generation, heating and cooling applications. In: Takahata K, editor. Micro electronic and mechanical systems. UK: In Tech; 2009. p. 15–24.

[178] Bilinsky-Slotylo VR, Vikhor LN, Mykhailovsky VY. Design of thermoelectric generator modules made of Mg and Mn silicide based materials. Thermoelectricity 2013:58–64.